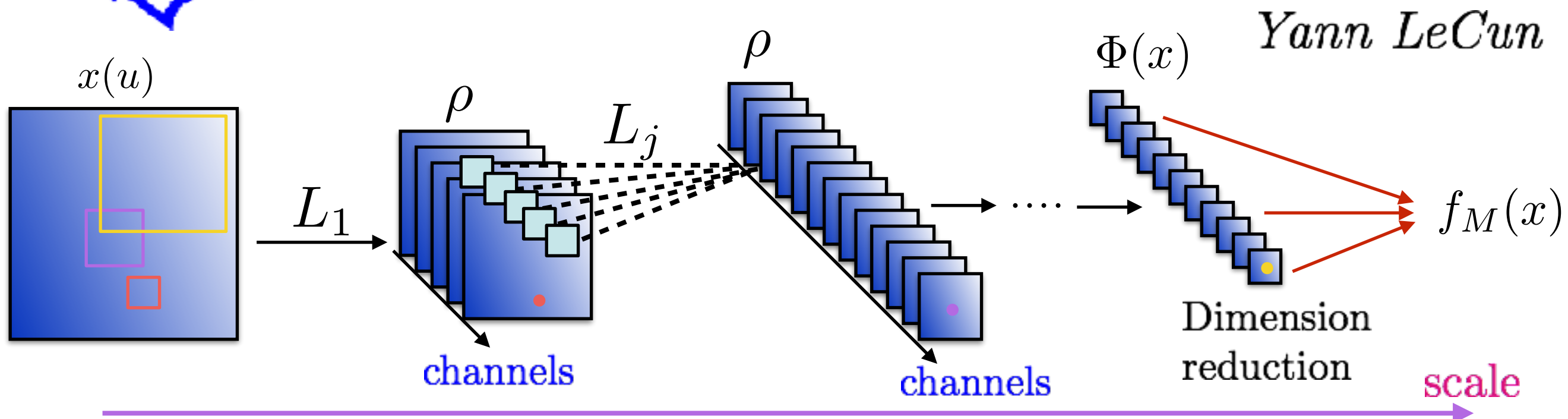


Unsupervised Learning and Inverse Problems with Deep Neural Networks

*Joan Bruna, Stéphane Mallat,
Ivan Dokmanic, Martin de Hoop*

École Normale Supérieure
www.di.ens.fr/data

Deep Convolutional Networks



L_j is a sum of spatial convolutions across channels, subsampling

$\rho(u)$ is a scalar non-linearity: $\max(u, 0)$ or $|u|$ or ...

.

Part I Architecture Simplification: wavelet scattering

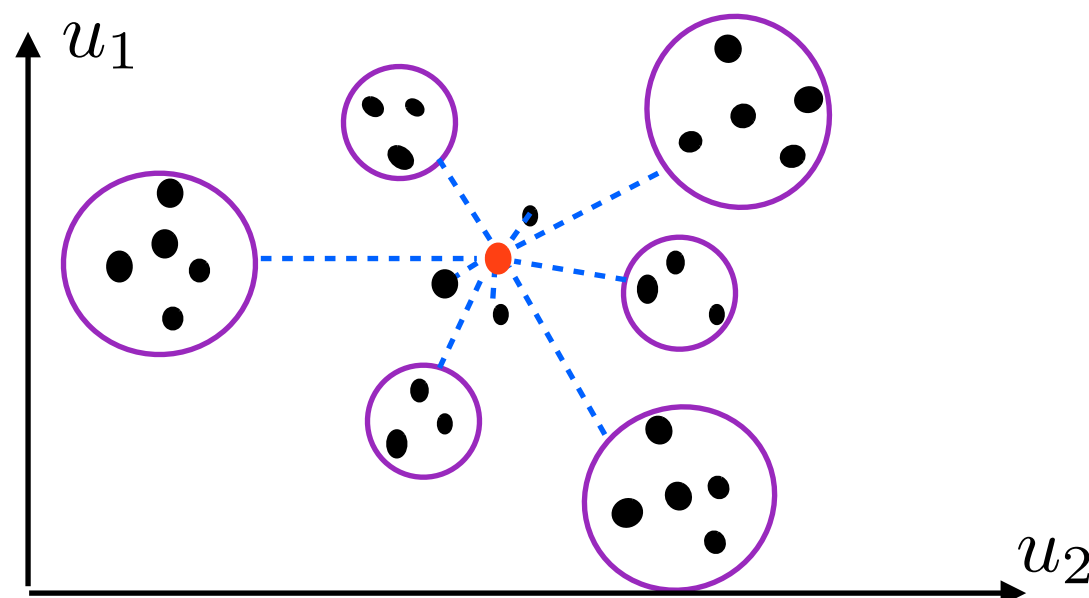
Part II Unsupervised learning: generative models

Part III Inverse problems

Dimensionality Reduction Multiscale

- Why can we learn despite the curse of dimensionality ?
Multiscale structures/interactions

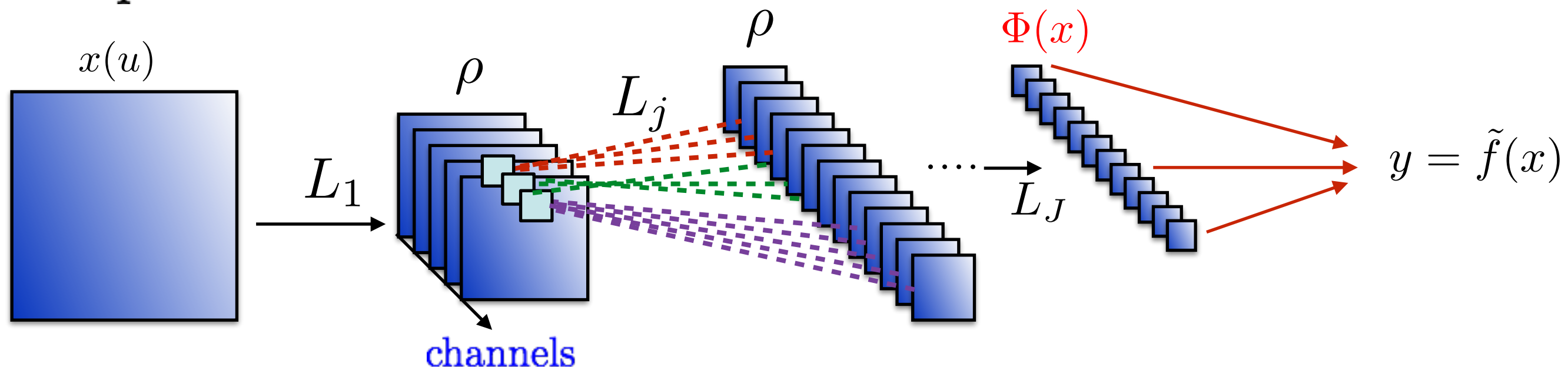
Interactions de d variables $x(u)$: pixels, particules, agents...



Regroupement of d interactions in $O(\log d)$

Deep Convolutional Trees

Simplified architecture:



Cascade of convolutions: no channel connections

predefined wavelet filters

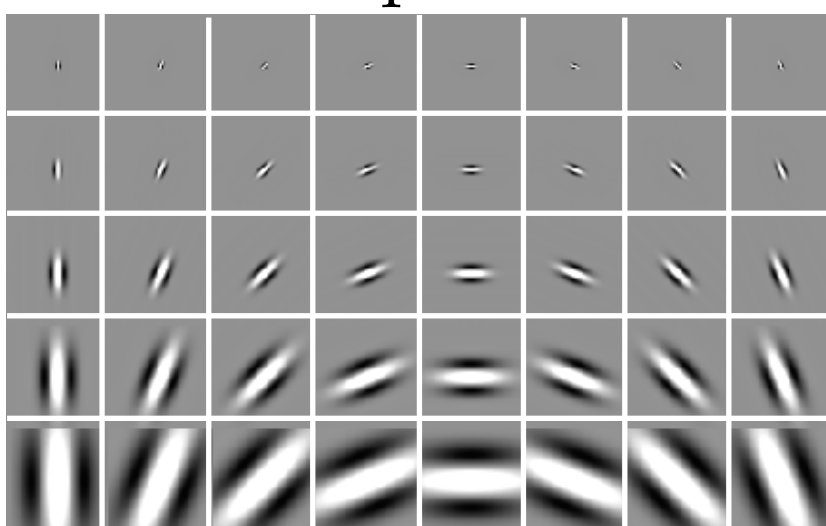
Scale separation with Wavelets

- Wavelet filter $\psi(u)$:

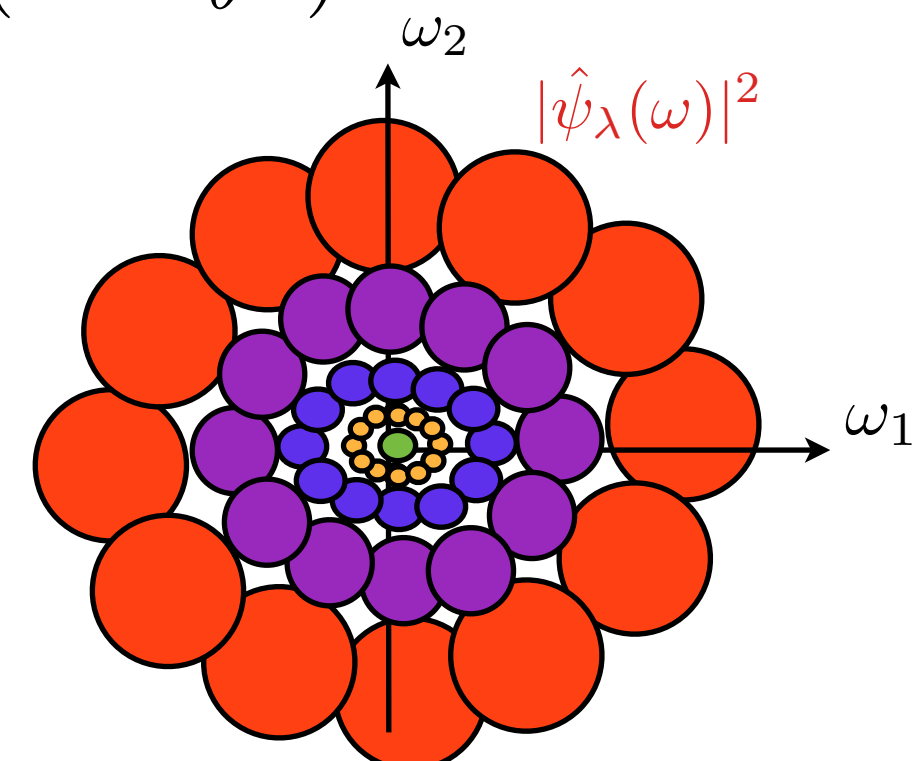
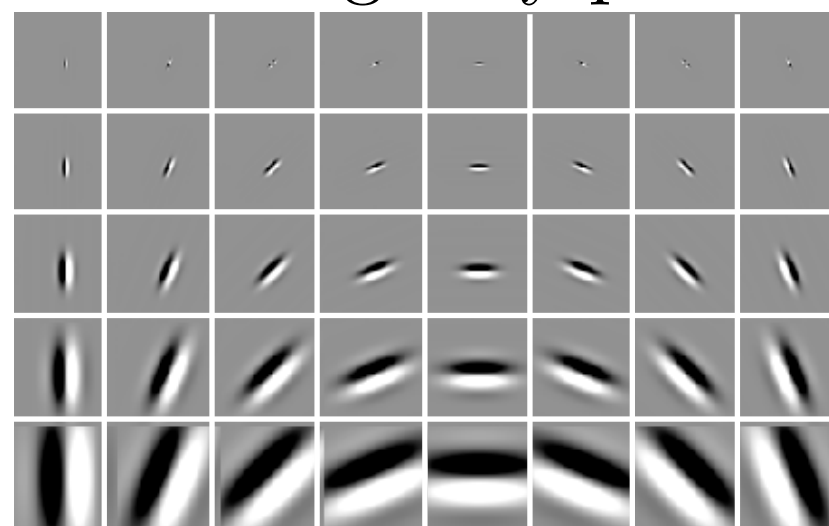


rotated and dilated: $\psi_{2^j, \theta}(u) = 2^{-j} \psi(2^{-j} r_\theta u)$

real parts



imaginary parts

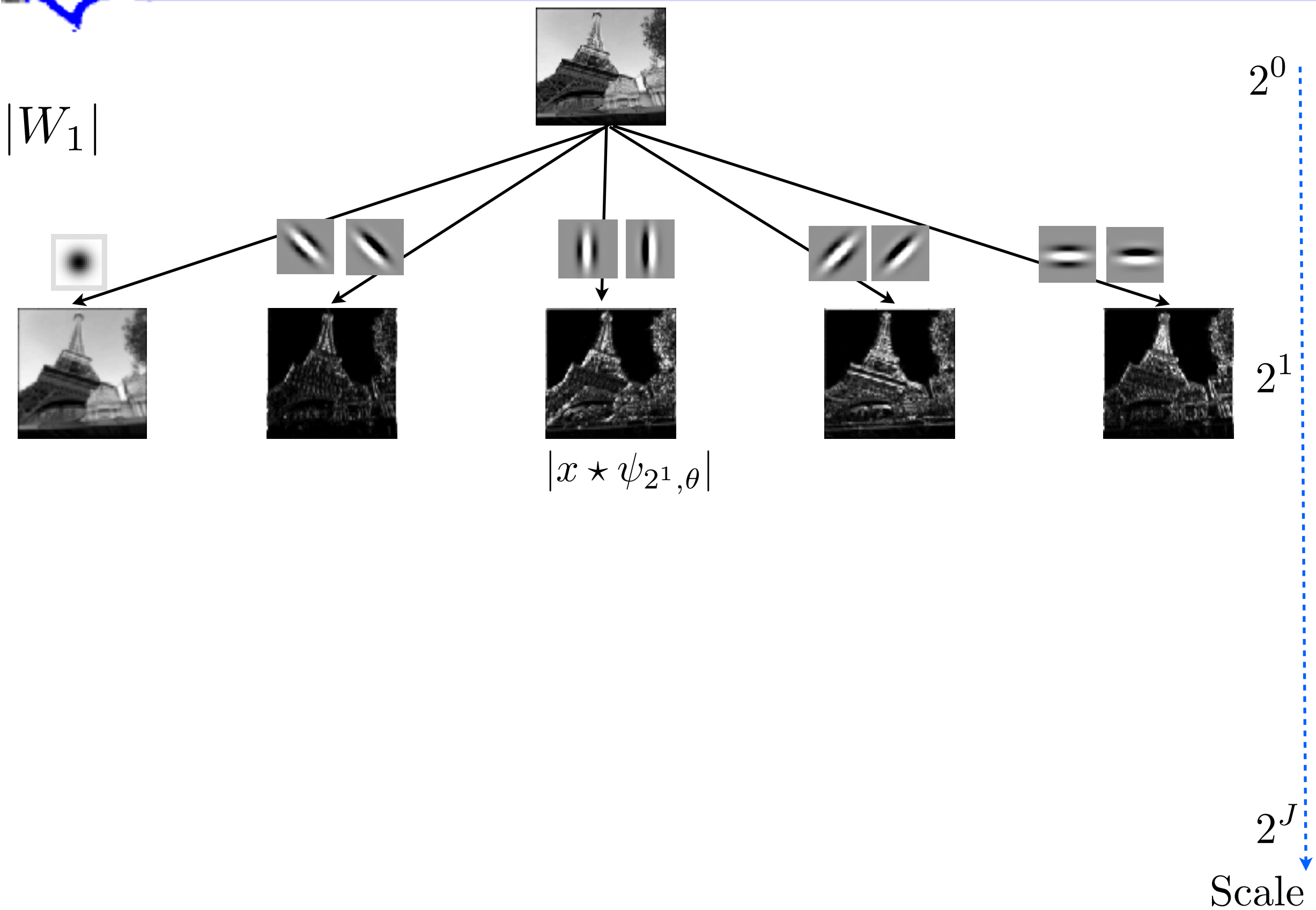


$$x \star \psi_{2^j, \theta}(u) = \int x(v) \psi_{2^j, \theta}(u - v) dv$$

- Wavelet transform: $Wx = \begin{pmatrix} x \star \phi_{2^J}(u) \\ x \star \psi_{2^j, \theta}(u) \end{pmatrix}_{j \leq J, \theta}$
- : average
: higher frequencies

Preserves norm: $\|Wx\|^2 = \|x\|^2$.

Fast Wavelet Filter Bank



Wavelet Filter Bank

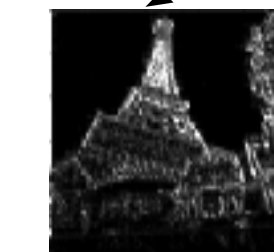
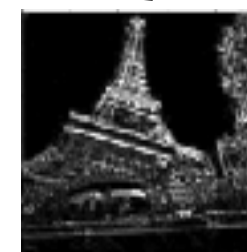
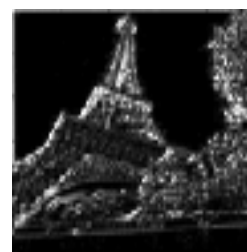
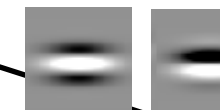
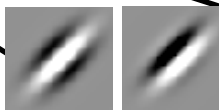
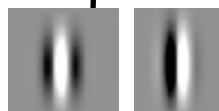
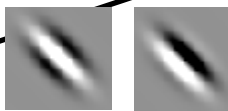
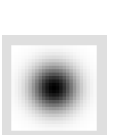
$$\rho(\alpha) = |\alpha|$$

$$|W_1|$$



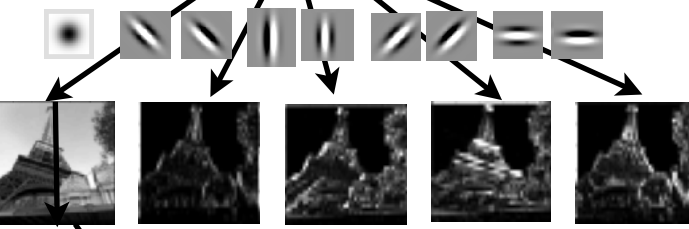
$$x(u)$$

$$2^0$$



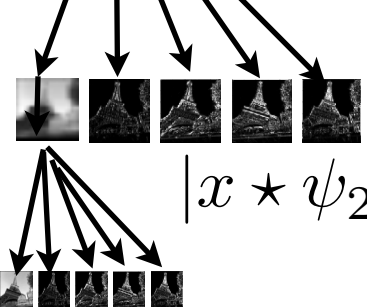
$$2^1$$

$$|x \star \psi_{2^1, \theta}|$$



$$|x \star \psi_{2^1, \theta}|$$

$$2^2$$

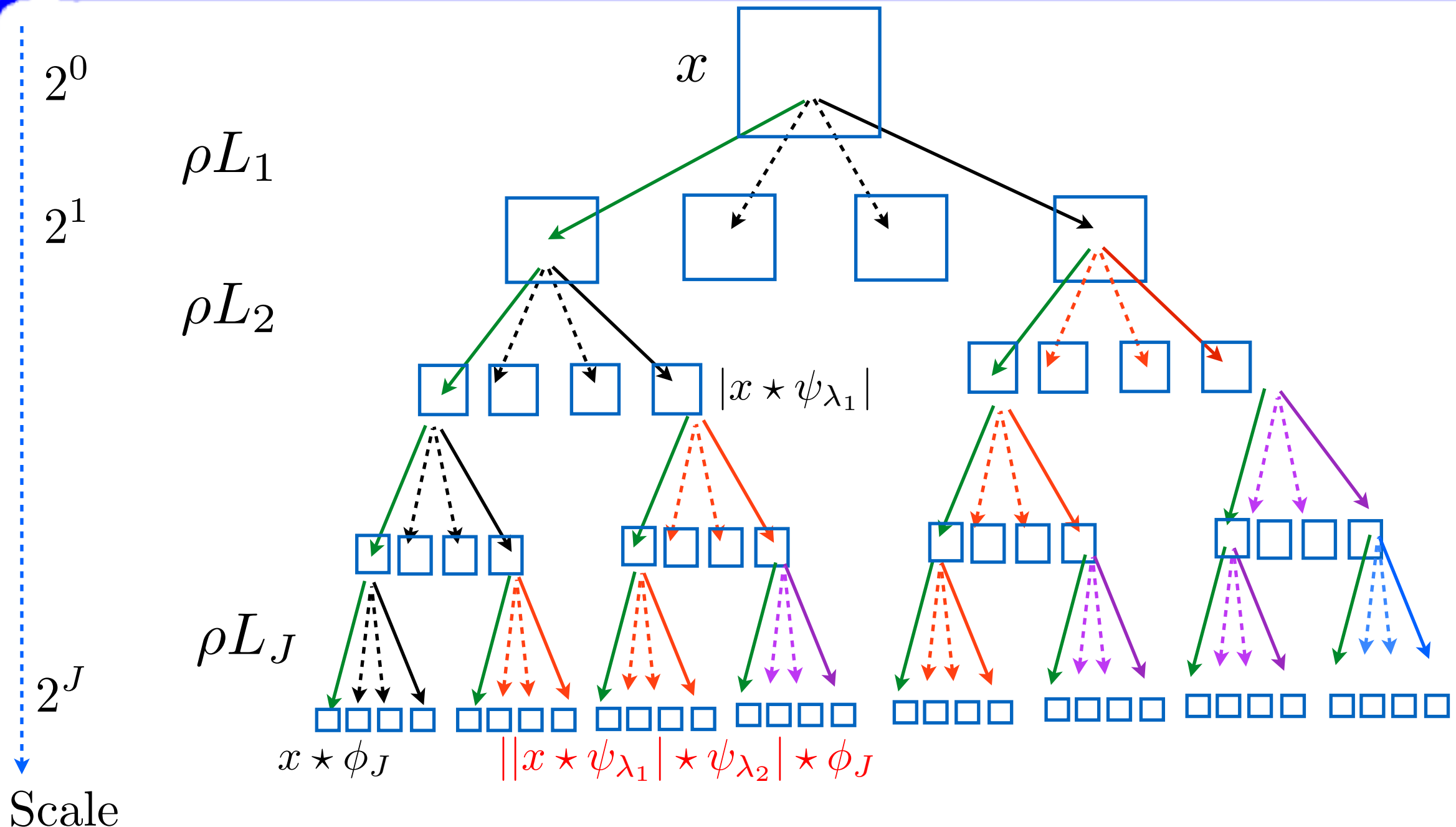


$$|x \star \psi_{2^j, \theta}|$$

$$2^J$$

Scale

Wavelet Scattering Network



$$S_J = \rho W_1 \quad \rho W_2 \quad \dots \quad \rho W_J$$

$$\rho(\alpha) = |\alpha| \quad S_J x = \left\{ ||| |x \star \psi_{\lambda_1}| \star \psi_{\lambda_2} \star \dots | \star \psi_{\lambda_m} | \star \phi_J \right\}_{\lambda_k}$$

Interactions across scales



Scattering Properties

$$S_J x = \begin{pmatrix} x \star \phi_{2^J} \\ |x \star \psi_{\lambda_1}| \star \phi_{2^J} \\ ||x \star \psi_{\lambda_1}| \star \psi_{\lambda_2}| \star \phi_{2^J} \\ |||x \star \psi_{\lambda_1}| \star \psi_{\lambda_2}| \star \psi_{\lambda_3}| \star \phi_{2^J} \\ \dots \end{pmatrix}_{\lambda_1, \lambda_2, \lambda_3, \dots} = \dots |W_3| |W_2| |W_1| x$$

Lemma: $\|x\|_{W_k D_\tau} = \|x\|_{W_k D_\tau W_k D_\tau W_k D_\tau W_k} \leq C' \|\nabla \tau\|_\infty$

Theorem: For appropriate wavelets, a scattering is

contractive $\|S_J x - S_J y\| \leq \|x - y\|$ (L^2 stability)

preserves norms $\|S_J x\| = \|x\|$

translations invariance and deformation stability:

if $D_\tau x(u) = x(u - \tau(u))$ then

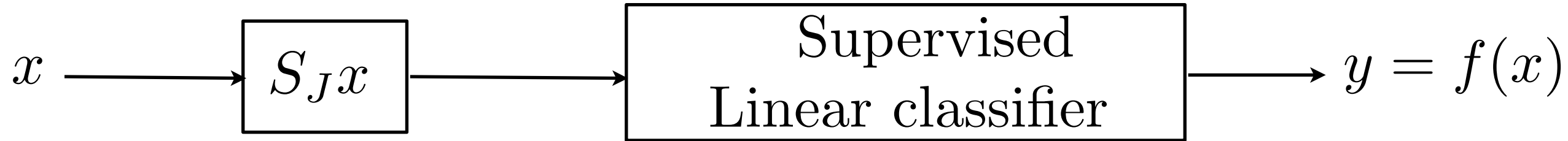
$$\lim_{J \rightarrow \infty} \|S_J D_\tau x - S_J x\| \leq C \|\nabla \tau\|_\infty \|x\|$$

Digit Classification: MNIST



3 6 8 / 7 9 b 6 9 1
6 7 5 7 8 6 3 4 8 5
2 1 7 9 7 1 2 8 7 6
4 8 1 9 0 1 8 8 9 4

Joan Bruna



Invariants to translations

Linearises small deformations

No learning

Invariants to specific deformations

Separates different patterns

Classification Errors

Training size	Conv. Net.	Scattering
50000	0.4%	0.4%

LeCun et. al.

Part II- Unsupervised Learning

joint work with Joan Bruna

Unsupervised learning:

Approximate the probability distribution $p(x)$ of $X \in \mathbb{R}^d$ given P realisations $\{x_i\}_{i \leq P}$ with potentially $P = 1$

Which class of processes can we approximate ?

Stationary Processes

- Ergodic versus non-ergodic (long-range dependance)
- Capture non-Gaussianity: geometry of realisations

Scattering/Deep Net. of a stationary process $X(t)$

$$S_J X = \begin{pmatrix} X \star \phi_{2^J}(t) \\ |X \star \psi_{\lambda_1}| \star \phi_{2^J}(t) \\ ||X \star \psi_{\lambda_1}| \star \psi_{\lambda_2}| \star \phi_{2^J}(t) \\ |||X \star \psi_{\lambda_2}| \star \psi_{\lambda_2}| \star \psi_{\lambda_3}| \star \phi_{2^J}(t) \\ \dots \end{pmatrix}_{\lambda_1, \lambda_2, \lambda_3, \dots} : \text{stationary vector}$$



Ergodicity and Moments

Scattering transform of a stationary vector $X \in \mathbb{R}^d$

maximum scale: $2^J = d$

$$S_J X = \begin{pmatrix} d^{-1} \sum_{u=1}^d X(u) \\ d^{-1} \|X \star \psi_{\lambda_1}\|_1 \\ d^{-1} \||X \star \psi_{\lambda_1}| \star \psi_{\lambda_2}\|_1 \\ d^{-1} \|||X \star \psi_{\lambda_2}| \star \psi_{\lambda_2}| \star \psi_{\lambda_3}\|_1 \\ \dots \end{pmatrix}_{\lambda_1, \lambda_2, \lambda_3, \dots}$$

$d \rightarrow \infty$

Central limit theorem
with "weak" ergodicity conditions

$$\mathbb{E}(SX) = \begin{pmatrix} \mathbb{E}(X) \\ \mathbb{E}(|X \star \psi_{\lambda_1}|) \\ \mathbb{E}(\||X \star \psi_{\lambda_1}| \star \psi_{\lambda_2}|) \\ \mathbb{E}(\|||X \star \psi_{\lambda_2}| \star \psi_{\lambda_2}| \star \psi_{\lambda_3}|) \\ \dots \end{pmatrix}_{\lambda_1, \lambda_2, \lambda_3, \dots} : \text{scattering moments.}$$

Generation of Random Processes

Scattering transform of a stationary vector $X \in \mathbb{R}^d$

maximum scale: $2^J = d$

$$S_J X = \begin{pmatrix} d^{-1} \sum_{u=1}^d X(u) \\ d^{-1} \|X \star \psi_{\lambda_1}\|_1 \\ d^{-1} \||X \star \psi_{\lambda_1}| \star \psi_{\lambda_2}\|_1 \\ d^{-1} \|||X \star \psi_{\lambda_2}| \star \psi_{\lambda_2}| \star \psi_{\lambda_3}\|_1 \\ \dots \end{pmatrix}_{\lambda_1, \lambda_2, \lambda_3, \dots}$$

- Reconstruction: compute \tilde{X} which satisfies

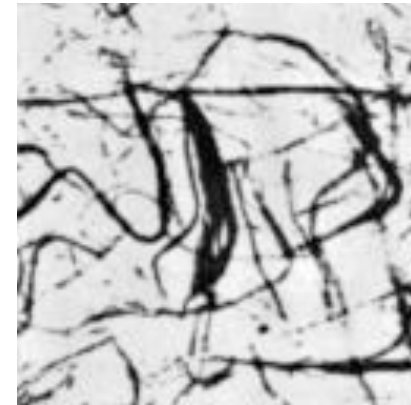
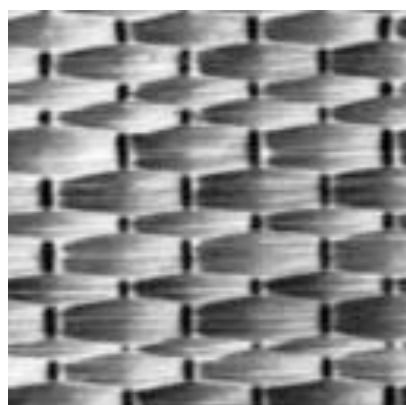
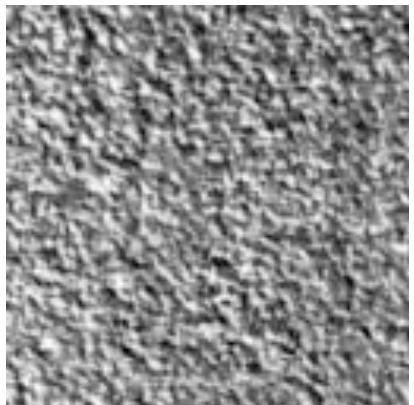
$$S_J \tilde{X} \approx S_J X$$

with random initialisation and gradient descent.

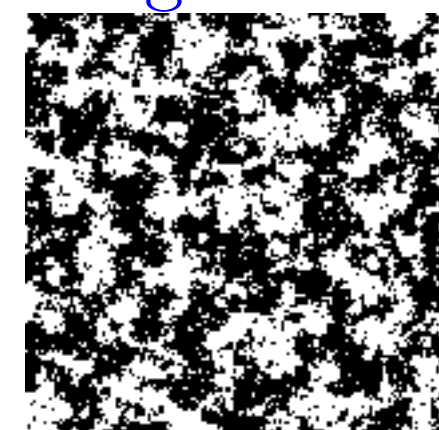
Texture Reconstructions

Joan Bruna

Texture of d pixels



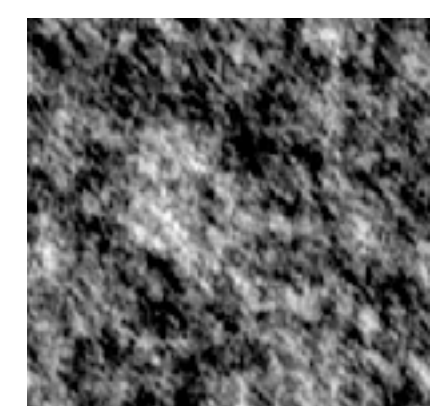
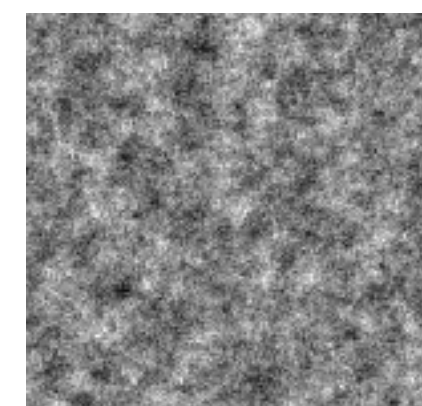
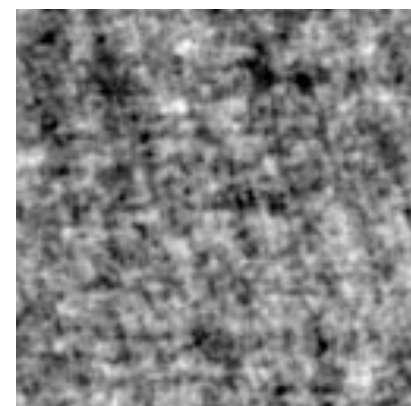
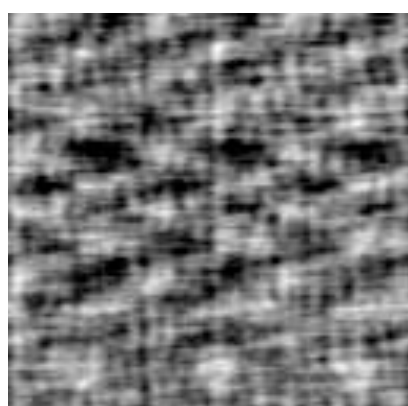
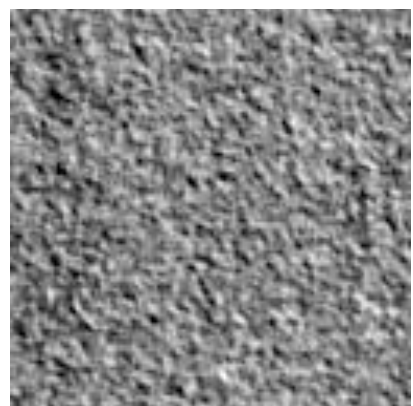
Statistical Physics
Ising-critical



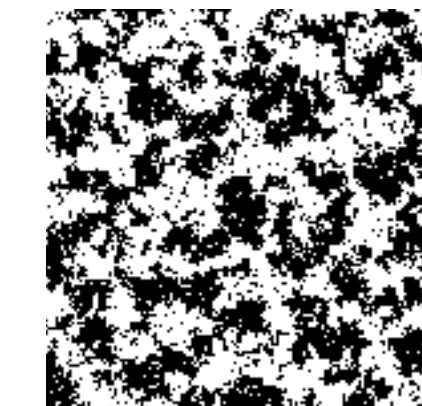
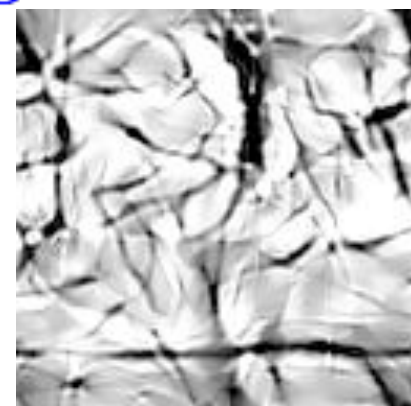
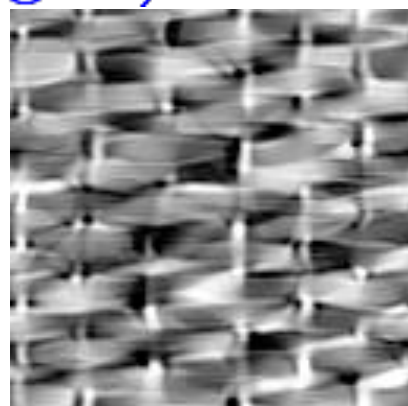
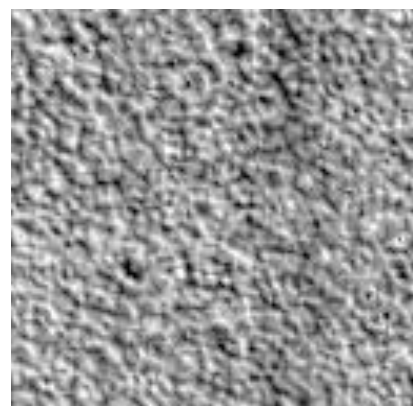
Turbulence 2D



Gaussian process model with d second order moments



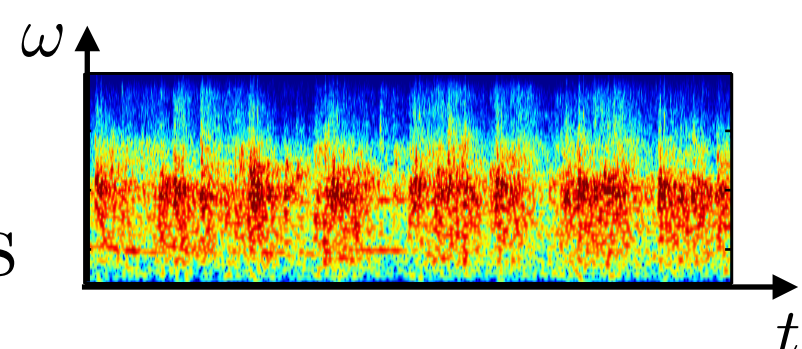
Reconstructions from $\|X \star \psi_{\lambda_1}\|_1$ and $\||X \star \psi_{\lambda_1}| \star \psi_{\lambda_2}\|_1$
 $O(\log^2 d)$ scattering coefficients



Representation of Audio Textures

Joan Bruna

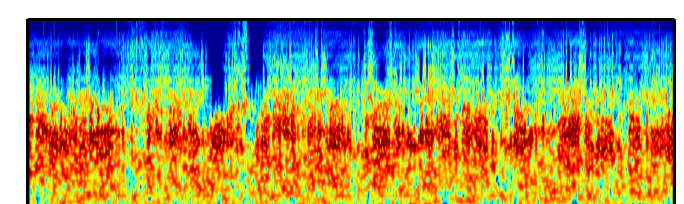
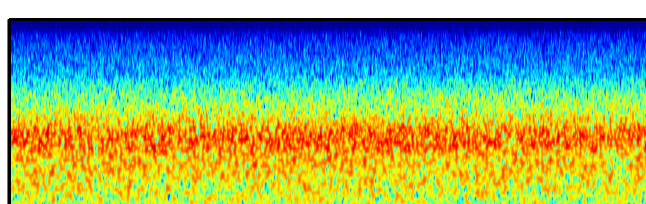
Original



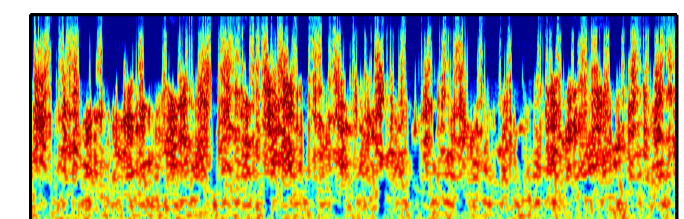
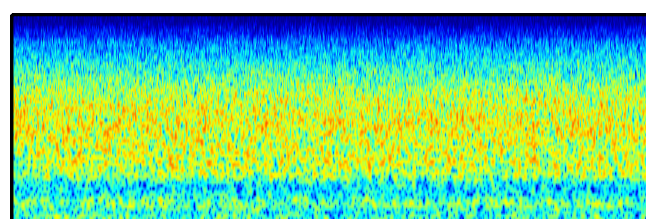
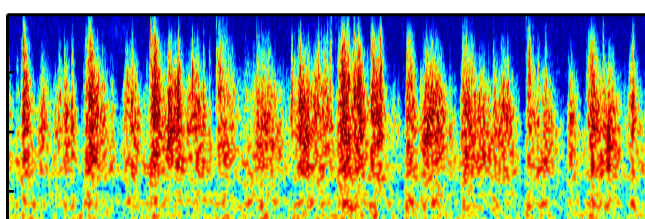
Gaussian
in time

Scattering
Order 2

Applauds



Paper



Cocktail Party

Max Entropy Canonical Models

- A representation $\Phi(x) = \{\phi_k(x)\}_{k \leq K}$ with $x \in \mathbb{R}^d$
- Canonical distribution $p(x)$ of X satisfies

$$\mu_k = \mathbb{E}(\phi_k X) = \int \phi_k(x) p(x) dx$$

with maximum entropy: $H(p) = - \int p(x) \log p(x) dx$

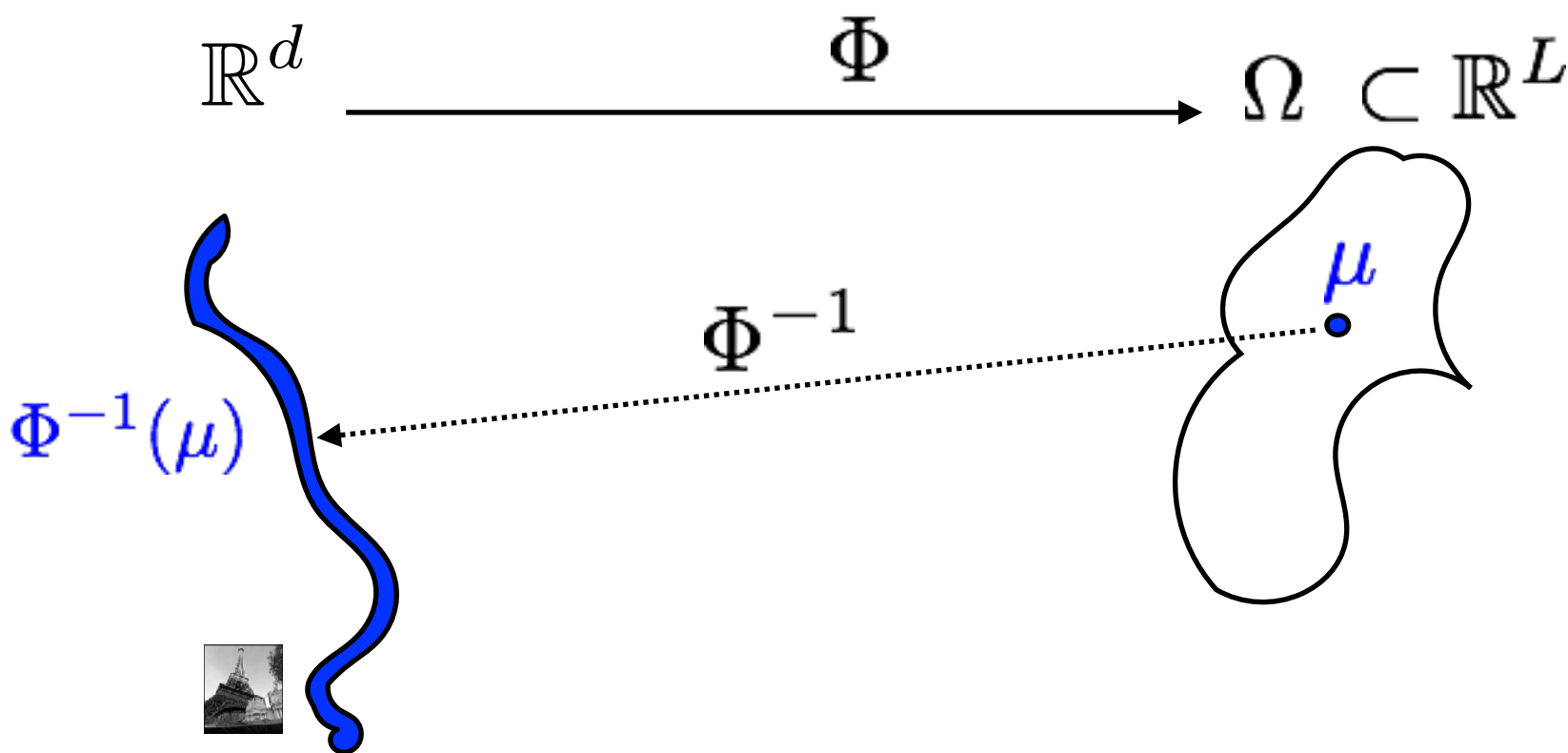
$$\Rightarrow p(x) = Z^{-1} \exp \left(- \sum_k \theta_k \phi_k(x) \right)$$

Gaussian, Markov random field models

- **Problem:** in other cases we can't compute the θ_k .

Ergodic Microcanonical Model

- If concentration: $\text{Prob}\left(|\Phi X - \mu| < \epsilon\right) \xrightarrow[d \rightarrow \infty]{} 1$
with $\mu = \mathbb{E}(\Phi X)$



A microcanonical model \tilde{X} has a distribution \tilde{p} of maximum entropy conditioned to $\Phi \tilde{X} = \mu$ which is uniform in $\Phi^{-1}(\mu)$ (if compact)

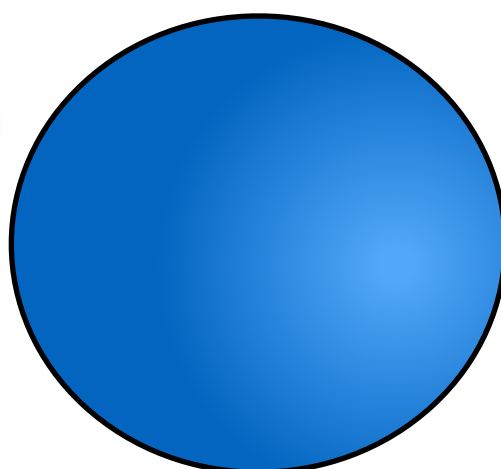
Uniform Distribution on Balls

- Sphere in \mathbb{R}^d

$$\Phi x = d^{-1/2} \|x\|_2 = \left(d^{-1} \sum_{k=1}^d |x(k)|^2 \right)^{1/2} = \mu$$

$\Phi^{-1}(\mu)$

not a low-dimensional
manifold !



Borel 1914

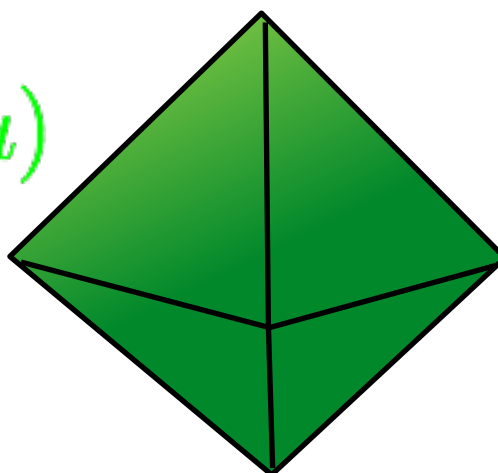
Diaconis, Freedman 1987

$$\tilde{X}(1), \dots, \tilde{X}(K) \xrightarrow[d \rightarrow \infty]{} \text{i.i.d Gaussian} \sim e^{-u^2/2\sigma^2}$$

- Simplex in \mathbb{R}^d

$$\Phi x = d^{-1} \|x\|_1 = d^{-1} \sum_{k=1}^d |x(k)| = \mu$$

$\Phi^{-1}(\mu)$



Diaconis, Freedman 1987

$$\tilde{X}(1), \dots, \tilde{X}(K) \xrightarrow[d \rightarrow \infty]{} \text{i.i.d Exponential} \sim e^{-\lambda|u|}$$

Scattering Representation

- Scattering coefficients of order 0, 1 and 2; up to scale 2^J

$$\Phi x = \left\{ d^{-1} \sum_u x(u) , d^{-1} \|x \star \psi_{\lambda_1}\|_1 , d^{-1} \||x \star \psi_{\lambda_1}| \star \psi_{\lambda_2}\|_1 \right\}$$

$\Phi^{-1}(\mu)$ is an intersection of about J^2 polytopes in \mathbb{R}^d

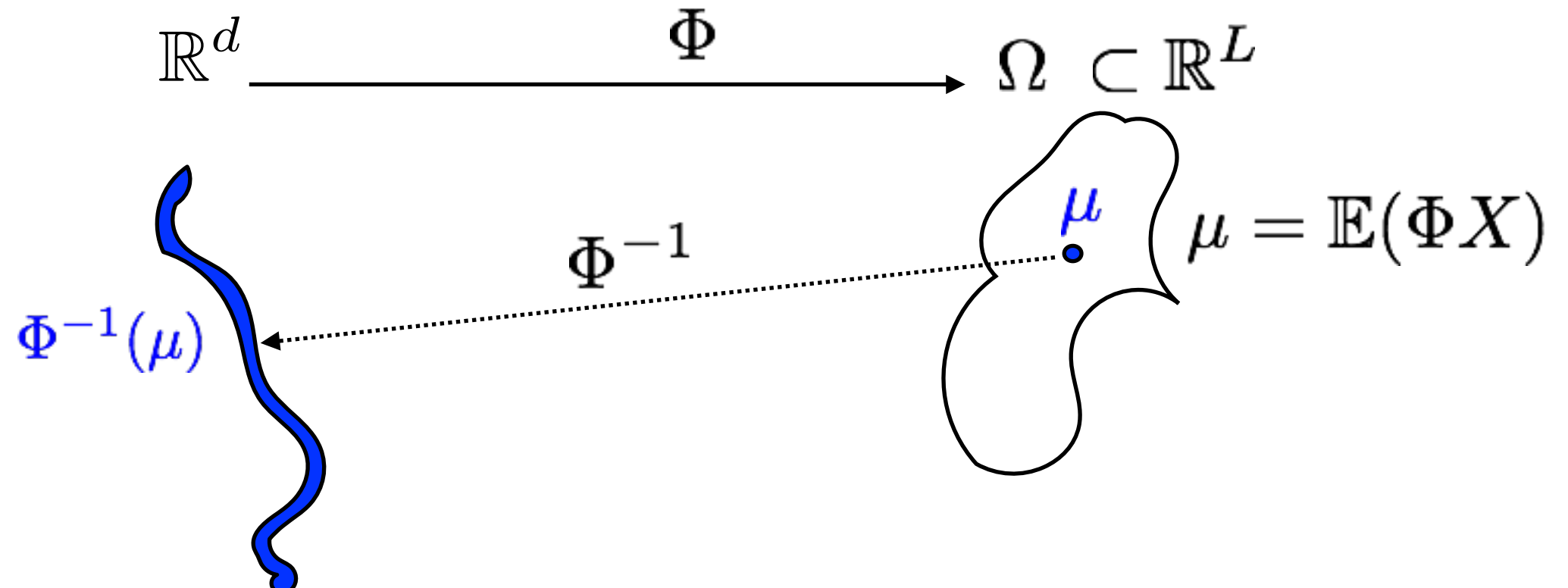
Complex high-dimensional geometry

- Reproduces ℓ^2 norms

$$d^{-1} \|x \star \psi_{\lambda_1}\|_2^2 = d^{-2} \|x \star \psi_{\lambda_1}\|_1^2 + \sum_{\lambda_2} d^{-2} \||x \star \psi_{\lambda_1}| \star \psi_{\lambda_2}\|_2^2 + \text{higher order}$$

Specify $\{\|x \star \psi_{\lambda_1}\|_2\}_{\lambda_1}$: intersection of ℓ^2 balls

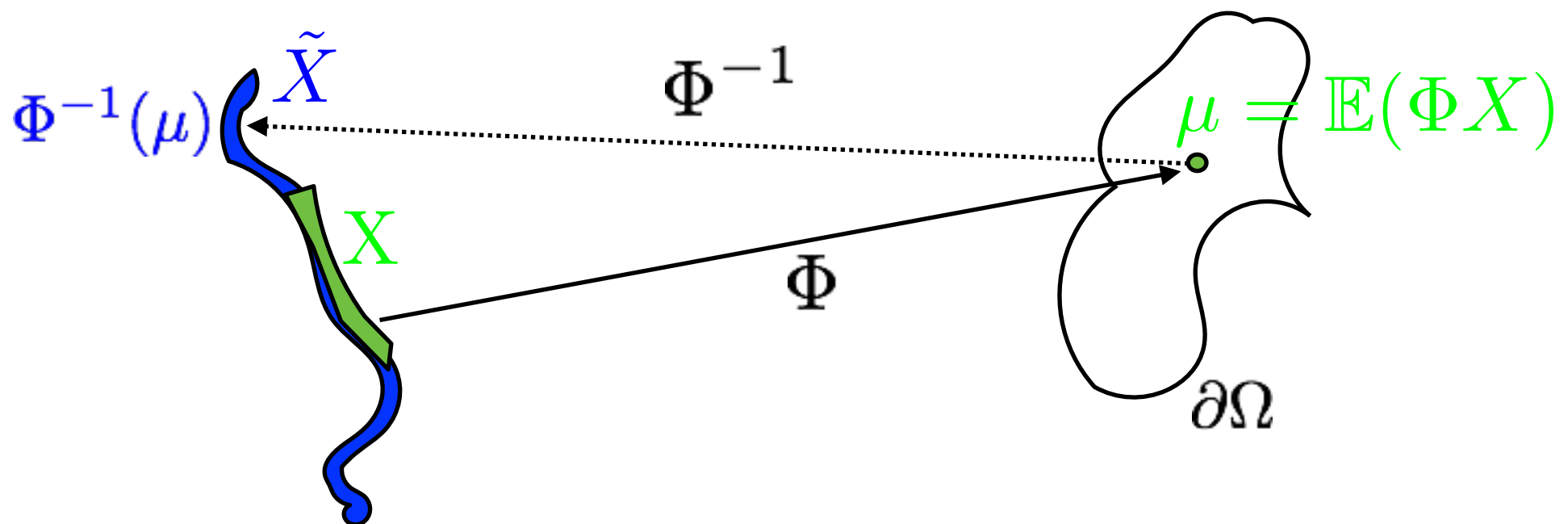
Microcanonical Scattering



Proposition If $X(u)$ is stationary and
 $X(u)$ and $X(v)$ are independent for $|u - v| \geq \Delta$

then $\lim_{d \rightarrow \infty} \mathbb{E}(\|\Phi X - \mu\|^2) = 0$

Scattering Approximations



Theorem If $X(u)$ is stationary and

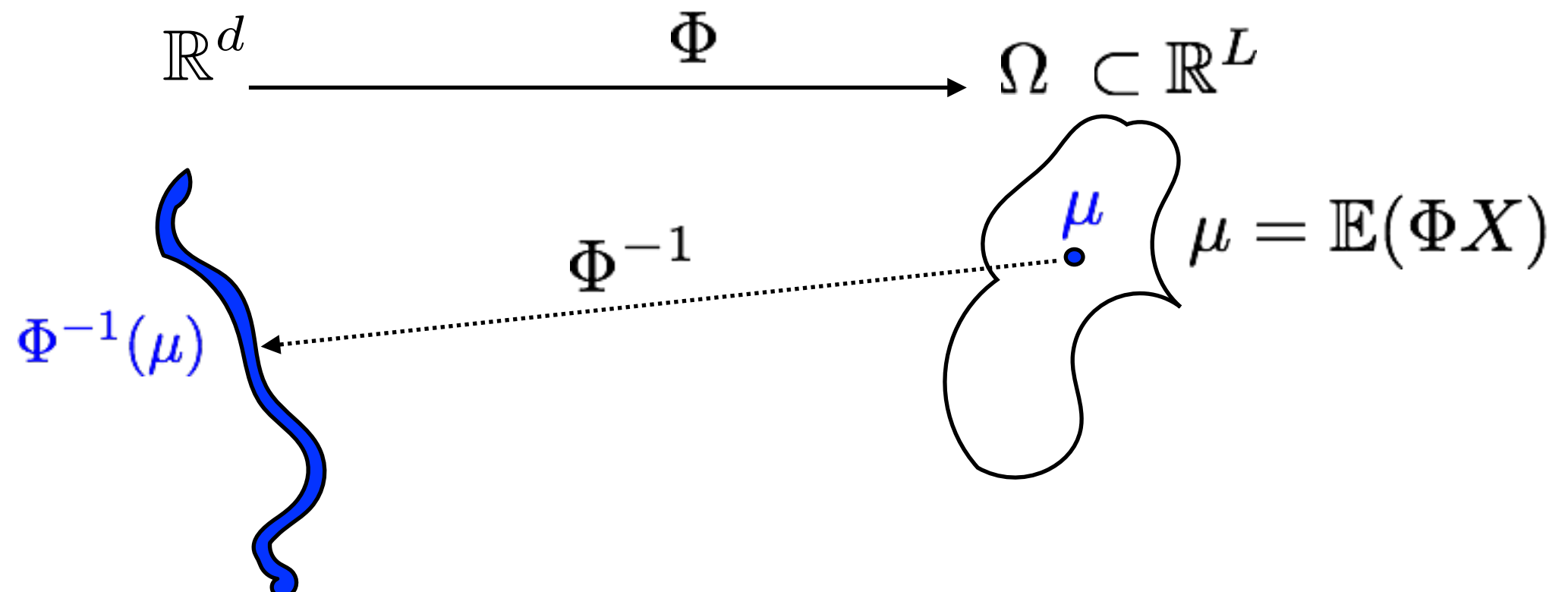
$X(u)$ and $X(v)$ are independent for $|u - v| \geq \Delta$

If Typical of \tilde{X} is typical of X

and $\lim_{d \rightarrow \infty} \mathbb{E}(|d^{-1} \log p(\tilde{X}) - H(p)|^2) = 0$ then

$\tilde{X}(1), \dots, \tilde{X}(K)$ converges in probability to $X(1), \dots, X(K)$

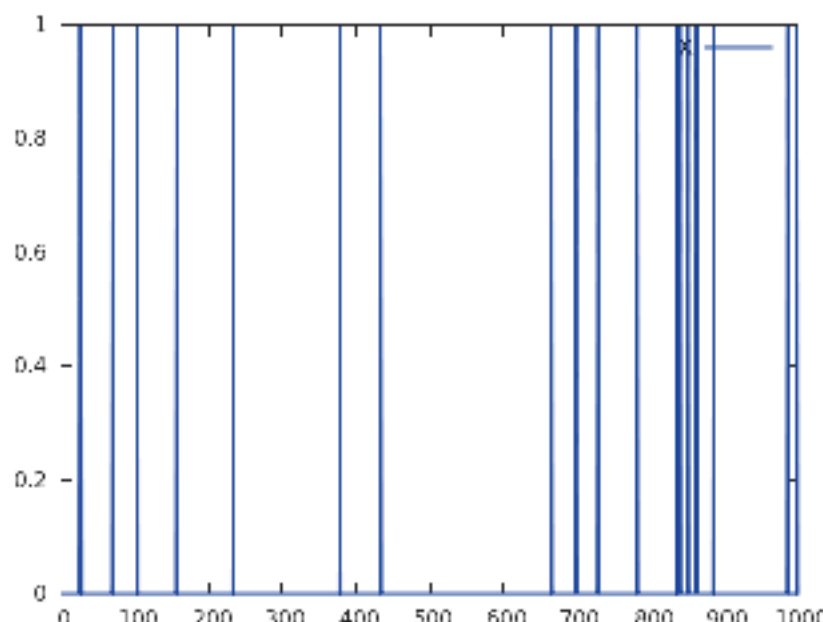
Ergodic Microcanonical Model



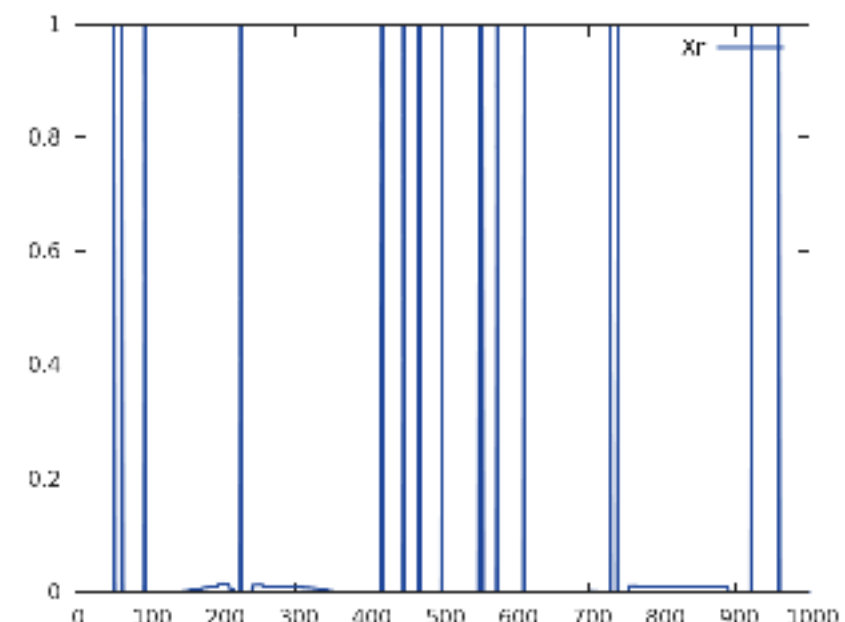
If X is Gaussian stationary
with a bounded and regular spectrum
then for a scattering with appropriate wavelets
 $\tilde{X}(1), \dots, \tilde{X}(K)$ converges in probability to $X(1), \dots, X(K)$
up to an arbitrary small error ϵ

Singular Ergodic Processes

Bernoulli X



Scattering Microcanonical \tilde{X}



Concentration of ΦX Typical of \tilde{X} is typical of X

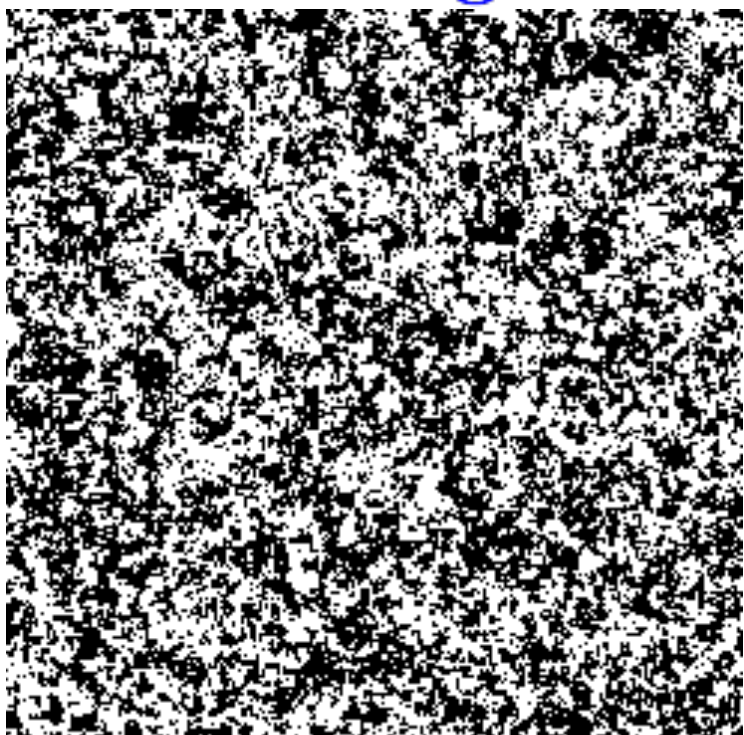
Why ?

Scattering Ising

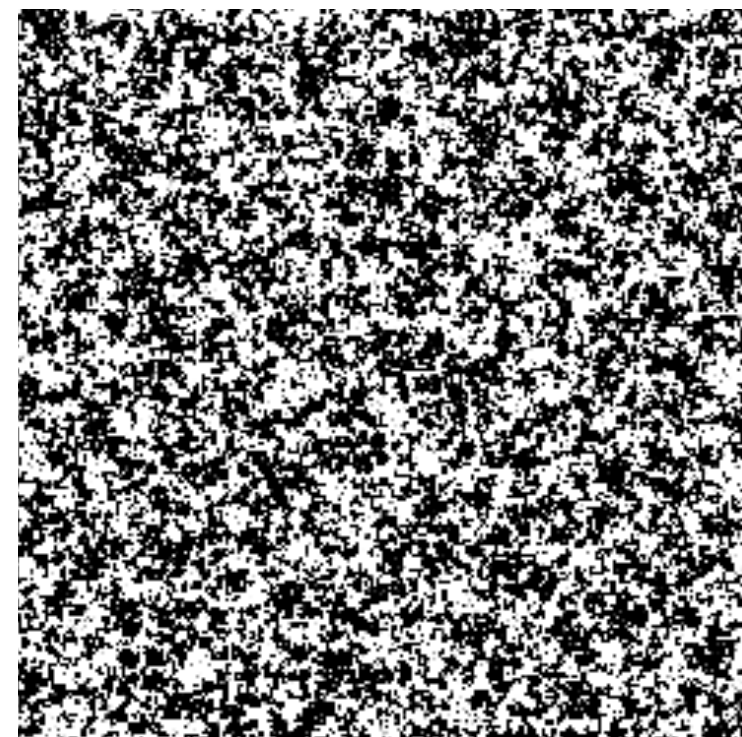
$$x(u) \in \{0, 1\}$$

$$p(x) = Z^{-1} \exp \left(\frac{1}{T} \sum_{(u,u') \in C_I} x(u) x(u') \right)$$

Ising X for $T \geq T_{critic}$
Ergodic



Microcanonical Scat \tilde{X}



Concentration of ΦX Typical of \tilde{X} is typical of X

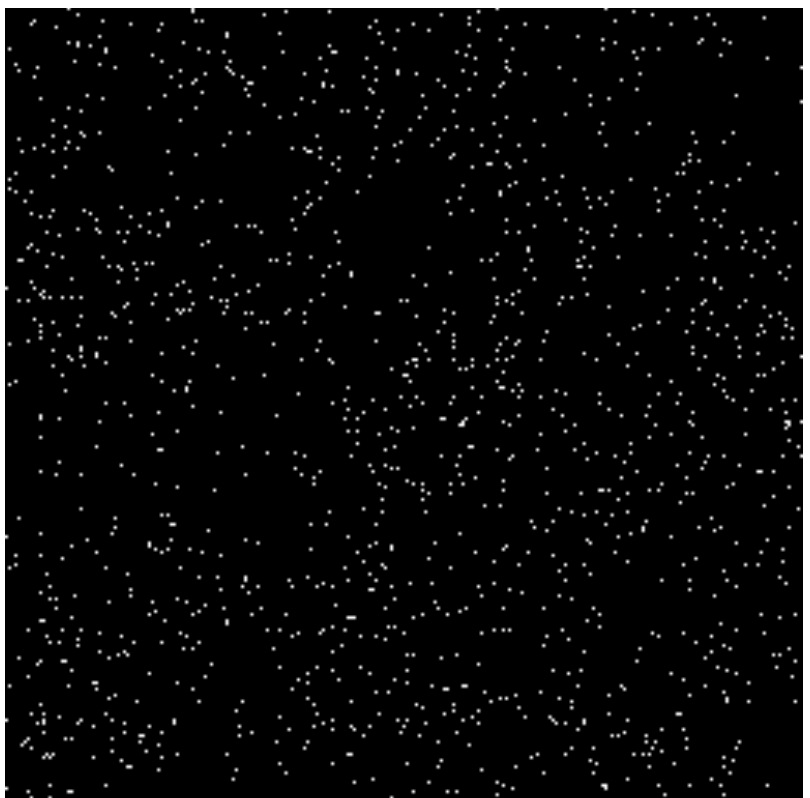
d	$\frac{\mathbb{E}(\ \Phi(X) - \mathbb{E}\Phi(X)\ ^2)}{\ \mathbb{E}\Phi(X)\ ^2}$	$\frac{\mathbb{E}(d^{-1} \log p(\tilde{X}) - H(p) ^2)}{H(p)^2}$
2^{12}	$3 \cdot 10^{-4}$	$1 \cdot 10^{-5}$
2^{14}	$1 \cdot 10^{-4}$	$5 \cdot 10^{-6}$

Why ?

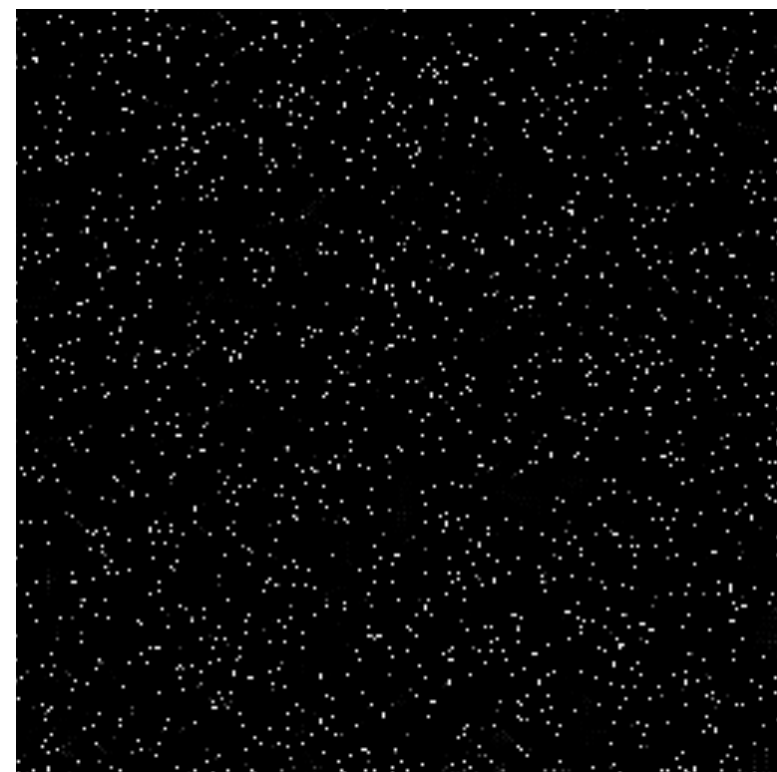
Stochastic Geometry: Cox Process

Bernoulli with random density $\lambda(u)$

Cox X Ergodic



Microcanonical Scat \tilde{X}



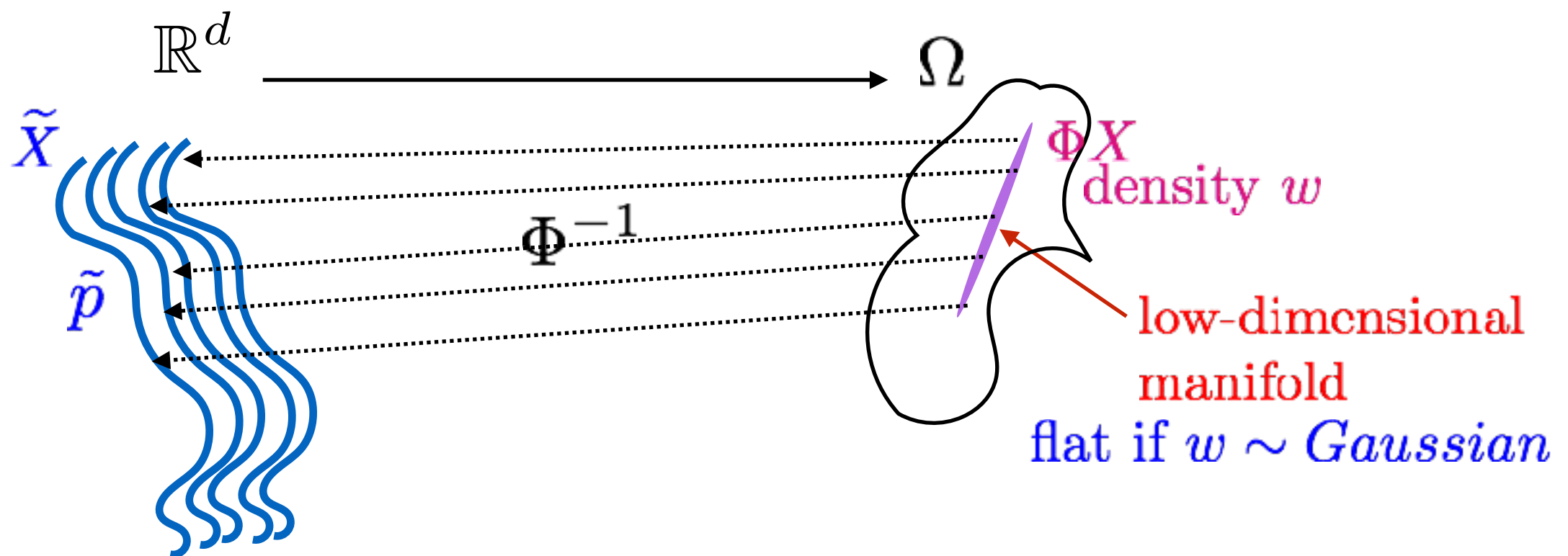
Concentration of ΦX

Typical of \tilde{X} is typical of X

d	$\frac{\mathbb{E}(\ \Phi(X) - \mathbb{E}\Phi(X)\ ^2)}{\ \mathbb{E}\Phi(X)\ ^2}$	$\frac{\mathbb{E}(d^{-1} \log p(\tilde{X}) - H(p) ^2)}{H(p)^2}$
2^{12}	$3 \cdot 10^{-4}$	
2^{14}	$1 \cdot 10^{-4}$	

Non-Ergodic Mixture

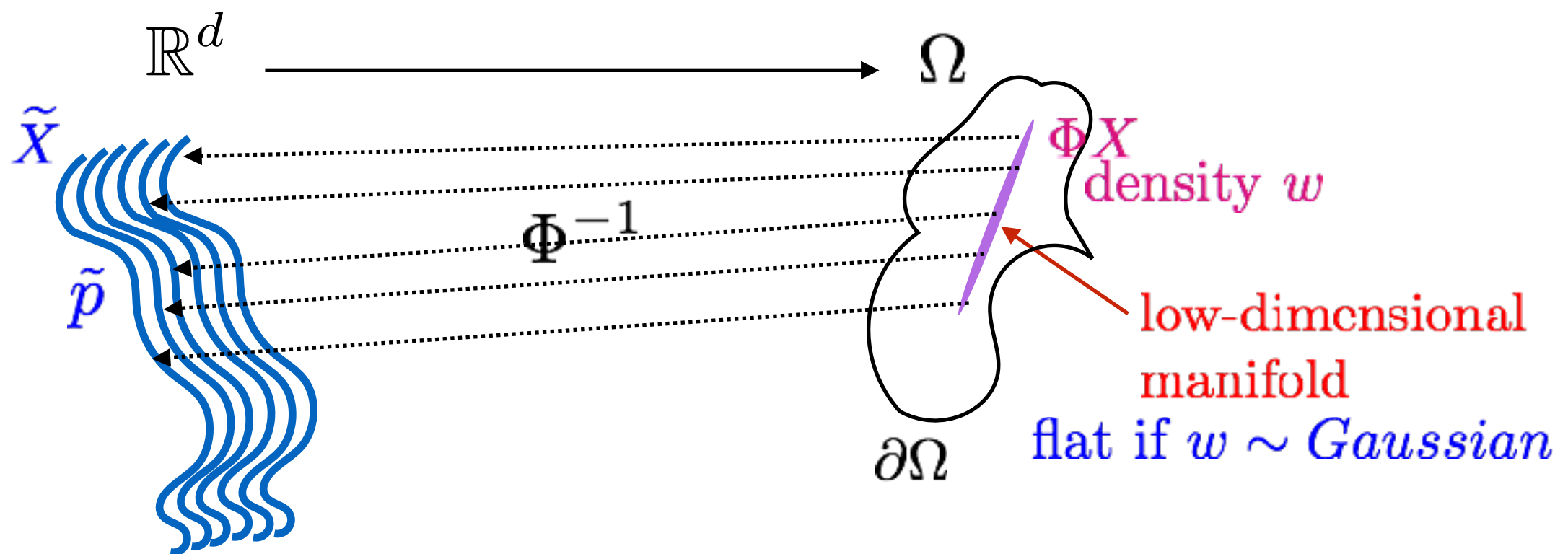
- Non-ergodicity: $\Phi(X)$ does not concentrate in all directions



Maximum entropy conditioned to $\Phi \tilde{X}$ having a density w
micro canonical mixture \tilde{X} weighted by the density w of ΦX

Non-Ergodic Microcanonical Mixture

- Non-ergodicity: $\Phi(X)$ does not concentrate in all directions



Theorem A microcanonical mixture has a density \tilde{p} with

$$\tilde{p}(x) = \frac{w(\Phi x)}{h(\Phi x)}$$

with $h(y) = \int_{\Phi^{-1}(y)} |J_L \Phi x|^{-1} d\mathcal{H}^{d-L}(x)$

which is singular only if $\Phi x \in \partial\Omega$

Scattering Multifractal Processes

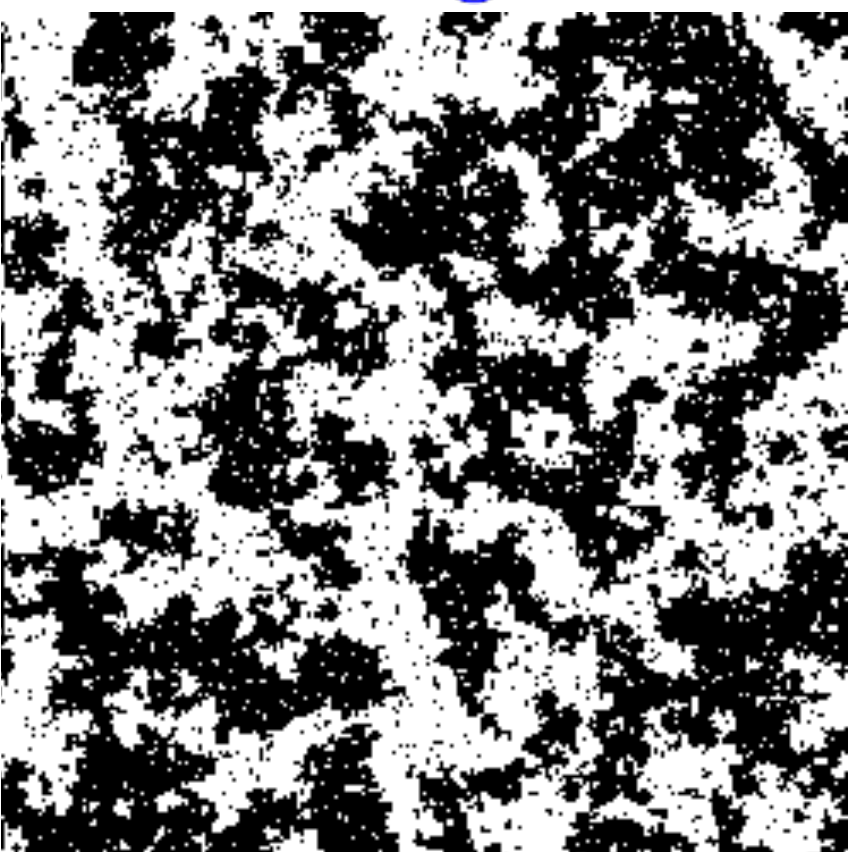
- Multifractal processes with stationary increment have non-ergodic low-frequencies: long-range correlations.
 - Wavelet coefficients $X \star \psi_\lambda(u)$ decorrelate at larger scales
 - Scattering coefficients of order 0, 1 and 2:

⇒ one-dimensional mixture weight w (non-ergodic part)
can be estimated from few examples: **manifold**.

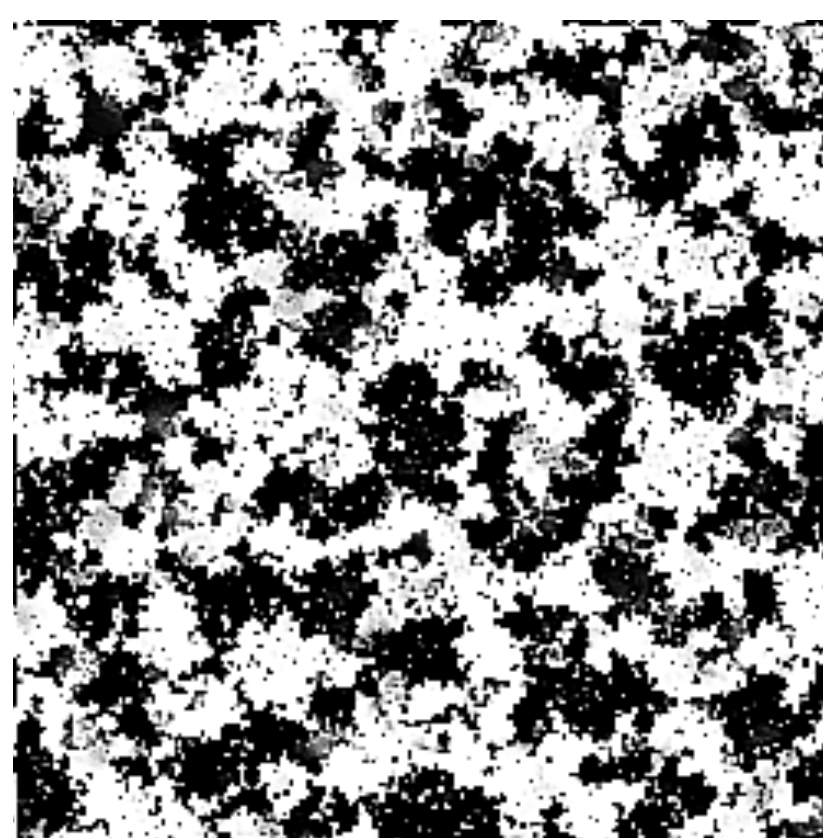
Scat Ising at Critical Temperature

$$p(x) = Z^{-1} \exp \left(\frac{1}{T} \sum_{(u,u') \in C_I} x(u) x(u') \right)$$

Ising X for $T = T_{critic}$
Non ergodic



Microcanonical Scat \tilde{X}

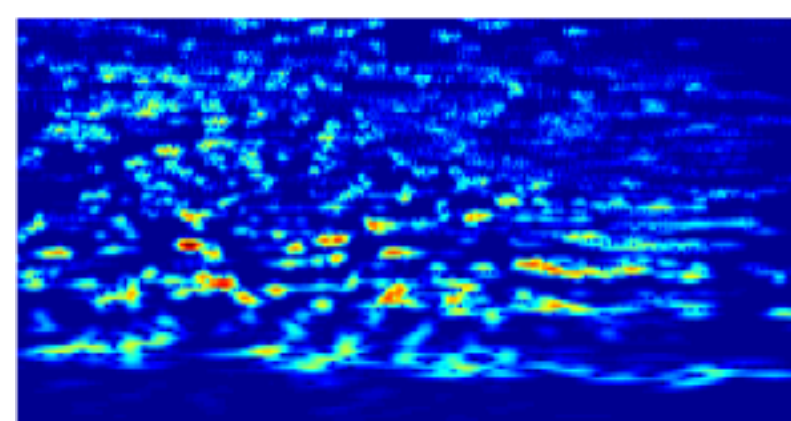
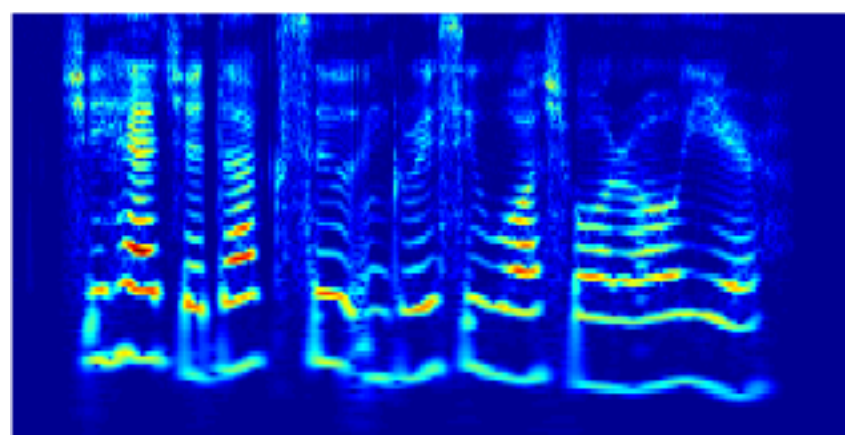
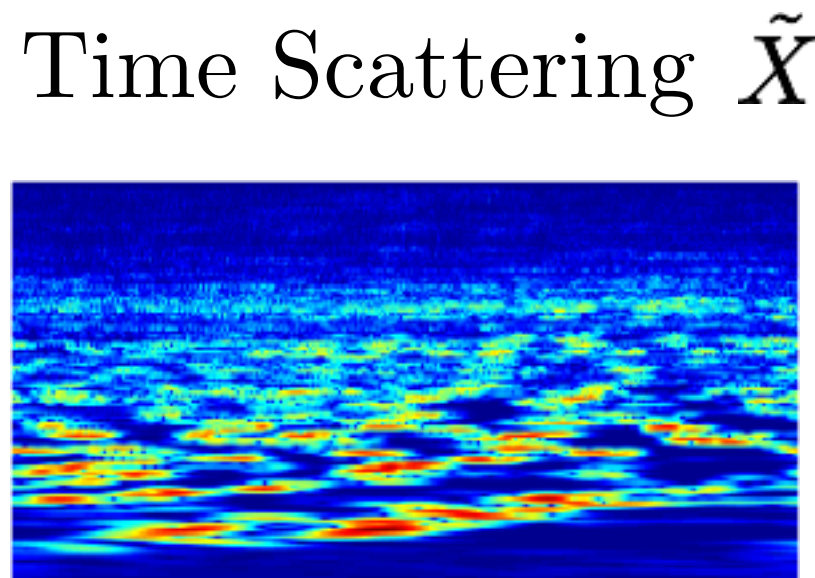
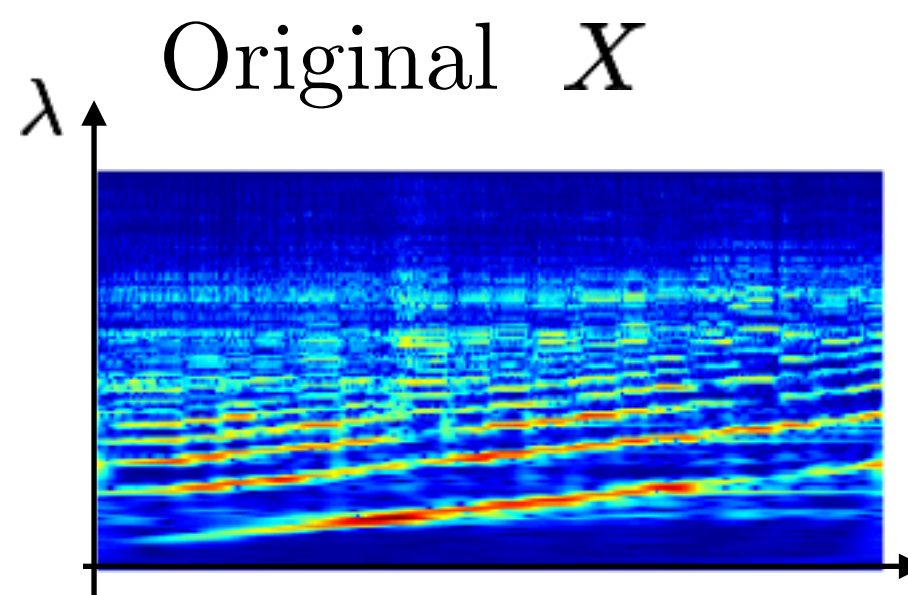


Concentration of ΦX without low-freq. Typical of \tilde{X} is typical of X

d	$\frac{\mathbb{E}(\ \Phi(X) - \mathbb{E}\Phi(X)\ ^2)}{\ \mathbb{E}\Phi(X)\ ^2}$	$\frac{\mathbb{E}(d^{-1} \log p(\tilde{X}) - H(p) ^2)}{H(p)^2}$
2^{12}	$8 \cdot 10^{-3}$	$2 \cdot 10^{-3}$
2^{14}	$2.5 \cdot 10^{-3}$	$2 \cdot 10^{-4}$

Failures of Audio Synthesis

J. Anden and V. Lostanlen

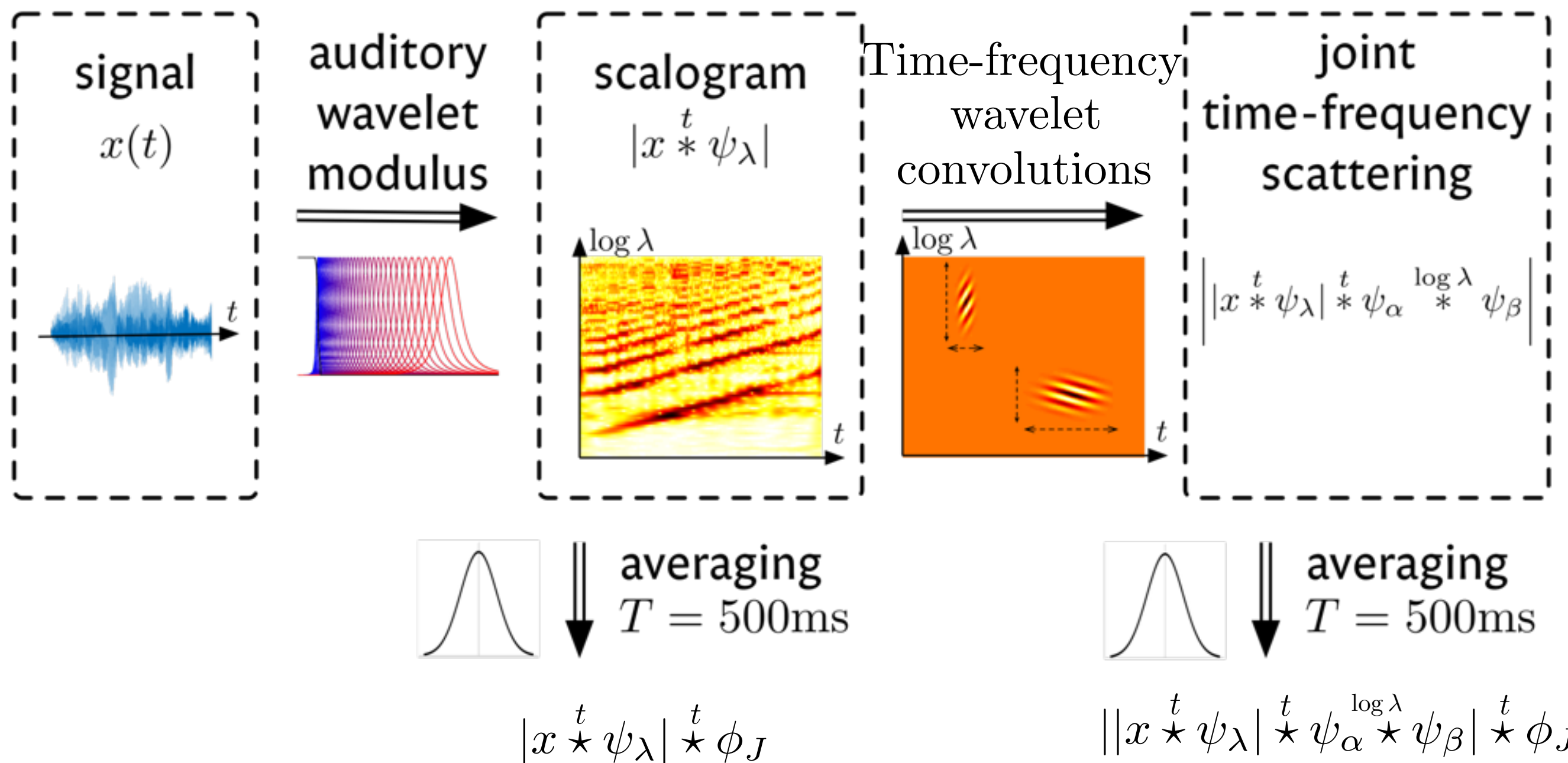


Typical of \tilde{X} is not typical of X

- Missing frequency connections \Rightarrow misalignments
- \Rightarrow incorporate two-dimensional translations in time-frequency

Time-Frequency Translation Group

J. Anden and V. Lostanlen



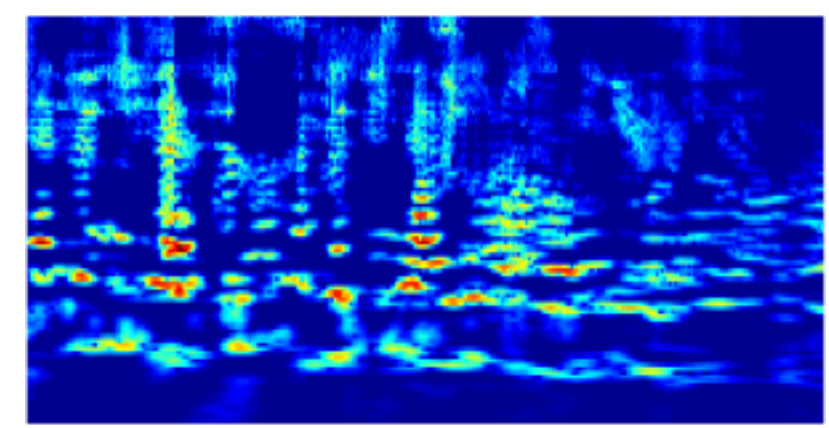
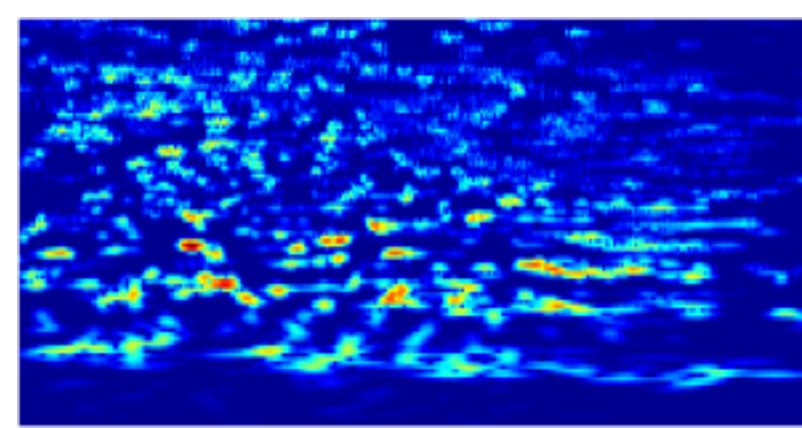
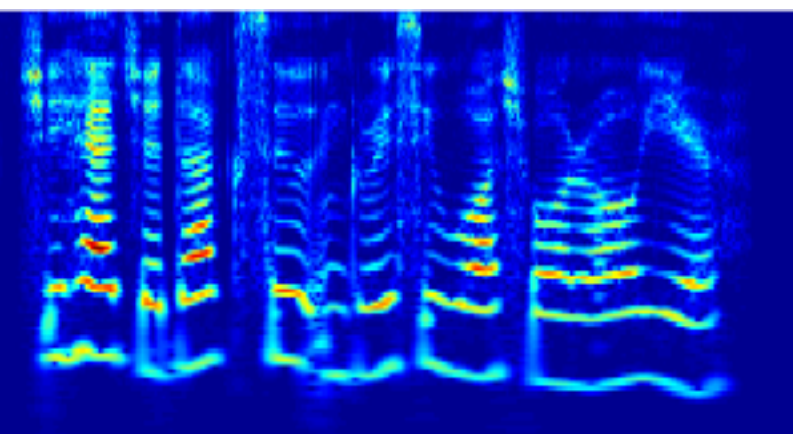
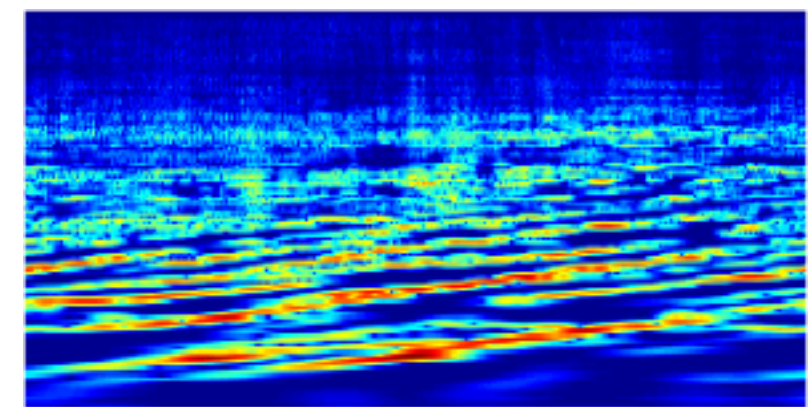
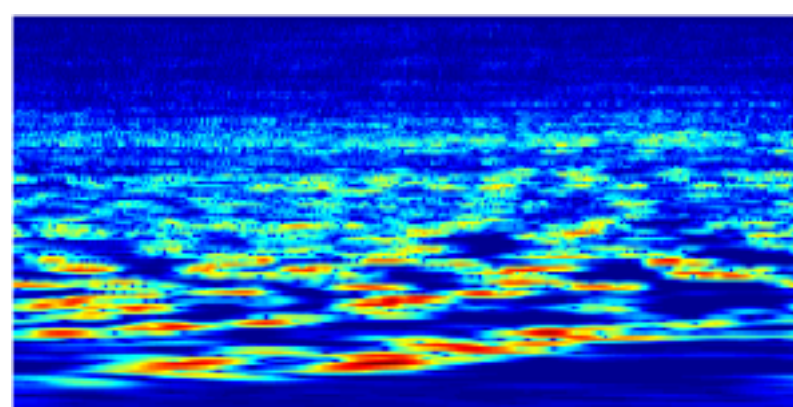
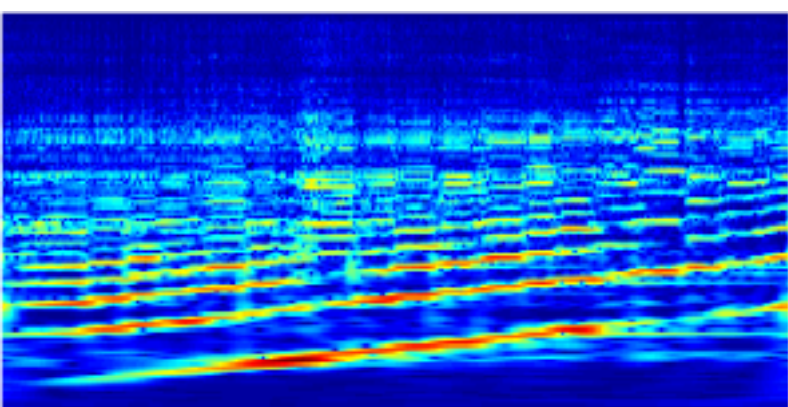
Joint Time-Frequency Scattering

J. Anden and V. Lostanlen

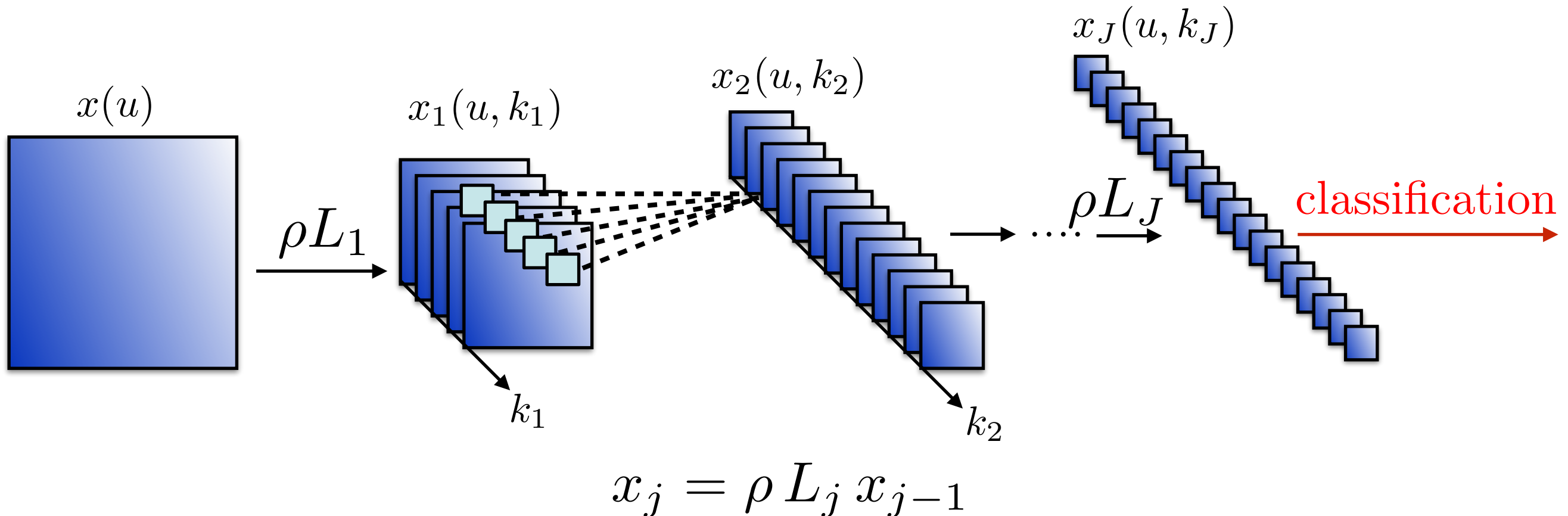
Original

Time Scattering

Time/Freq Scattering



Part III- Supervised Learning



- L_j is a linear combination of convolutions and subsampling:

$$x_j(u, k_j) = \rho \left(\sum_k x_{j-1}(\cdot, k) \star h_{k_j, k}(u) \right)$$

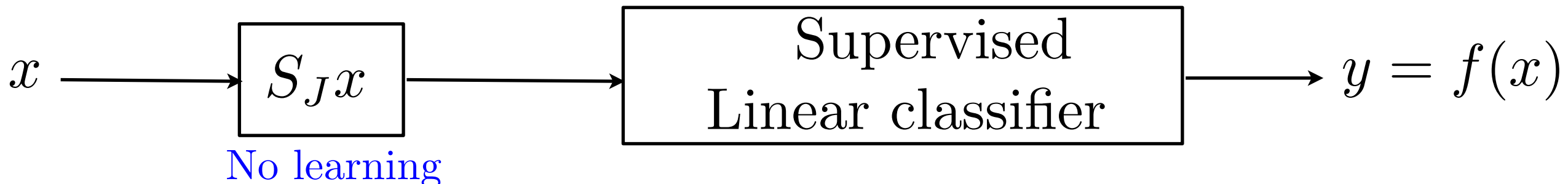
sum across channels

What is the role of channel connections ?

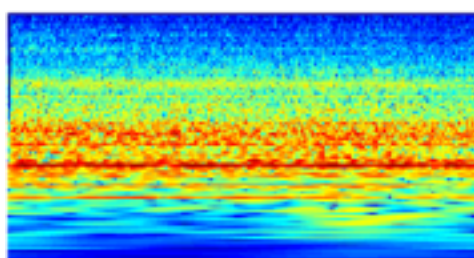
Invariant over groups of operators other than translations

Environmental Sound Classification

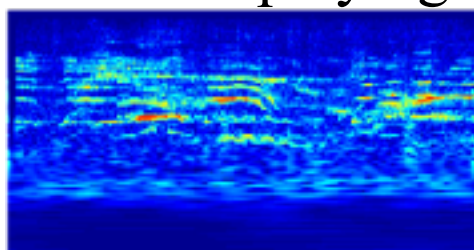
J. Anden and V. Lostanlen



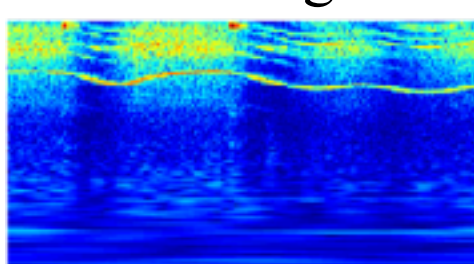
air conditioner



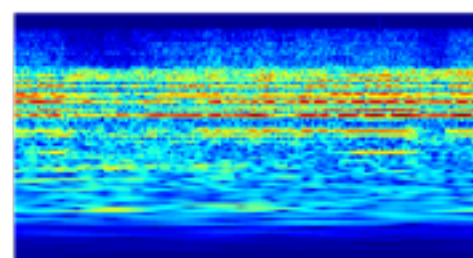
children playing



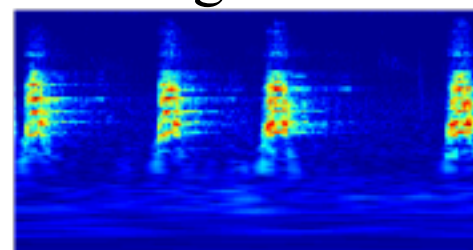
drilling



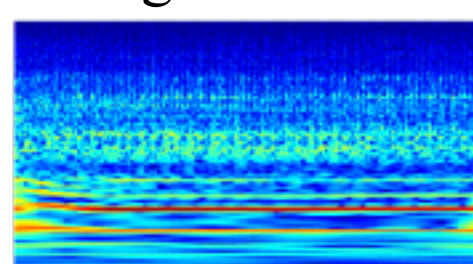
car horns



dog barks



engine at idle



UrbanSound8k: 10 classes
8k training examples
class-wise average error

MFCC audio descriptors	0,39
time scattering	0,27
ConvNet (Piczak, MLSP 2015)	0,26
time-frequency scattering	0,2

Inverse Scattering Transform

Joan Bruna

- Given $S_J x$ we want to compute \tilde{x} such that:

$$S_J \tilde{x} = \begin{pmatrix} \tilde{x} \star \phi_{2^J} \\ |\tilde{x} \star \psi_{\lambda_1}| \star \phi_{2^J} \\ \dots \\ |||\tilde{x} \star \psi_{\lambda_1}| \star ..| \star \psi_{\lambda_m}| \star \phi_{2^J} \end{pmatrix}_{\lambda_1, \dots, \lambda_m} = \begin{pmatrix} x \star \phi_{2^J} \\ |x \star \psi_{\lambda_1}| \star \phi_{2^J} \\ \dots \\ |||x \star \psi_{\lambda_1}| \star ..| \star \psi_{\lambda_m}| \star \phi_{2^J} \end{pmatrix}_{\lambda_1, \dots, \lambda_m} = S_J x$$

We shall use $m = 2$.

- If $x(u)$ is a Dirac, or a straight edge or a sinusoid then \tilde{x} is equal to x up to a translation.

Sparse Shape Reconstruction

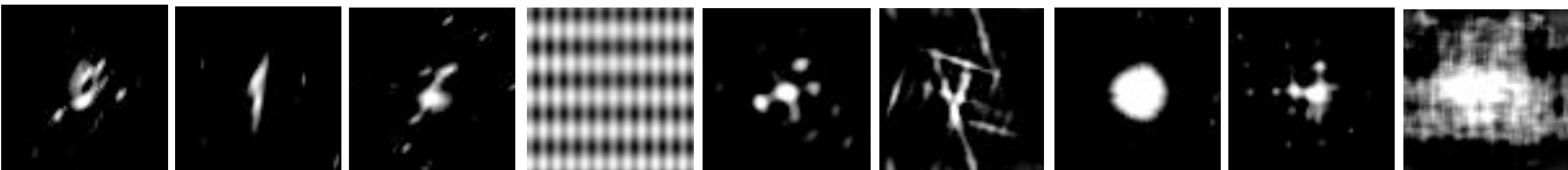
Joan Bruna

With a gradient descent algorithm:

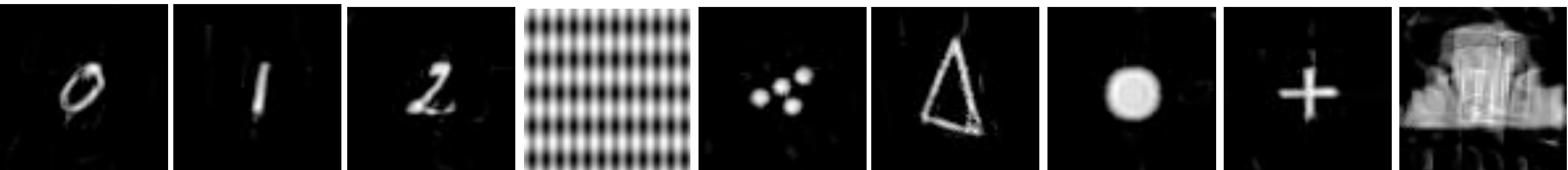
Original images of N^2 pixels:



$m = 1, 2^J = N$: reconstruction from $O(\log_2 N)$ scattering coeff.



$m = 2, 2^J = N$: reconstruction from $O(\log_2^2 N)$ scattering coeff.



Multiscale Scattering Reconstructions

Original
Images

N^2 pixels

Scattering
Reconstruction

$$2^J = 16$$

$1.4 N^2$ coeff.

$$2^J = 32$$

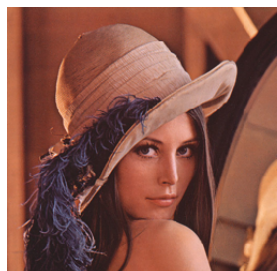
$0.5 N^2$ coeff.

$$2^J = 64$$

$$2^J = 128 = N$$



III- Inverse Problems

 x

$$\xrightarrow{F}$$

 y

- Best Linear Method: Least Squares estimate (linear interpolation):

$$\hat{y} = (\hat{\Sigma}_x^\dagger \hat{\Sigma}_{xy})x$$

Super-Resolution

 x

$$\xrightarrow{F}$$

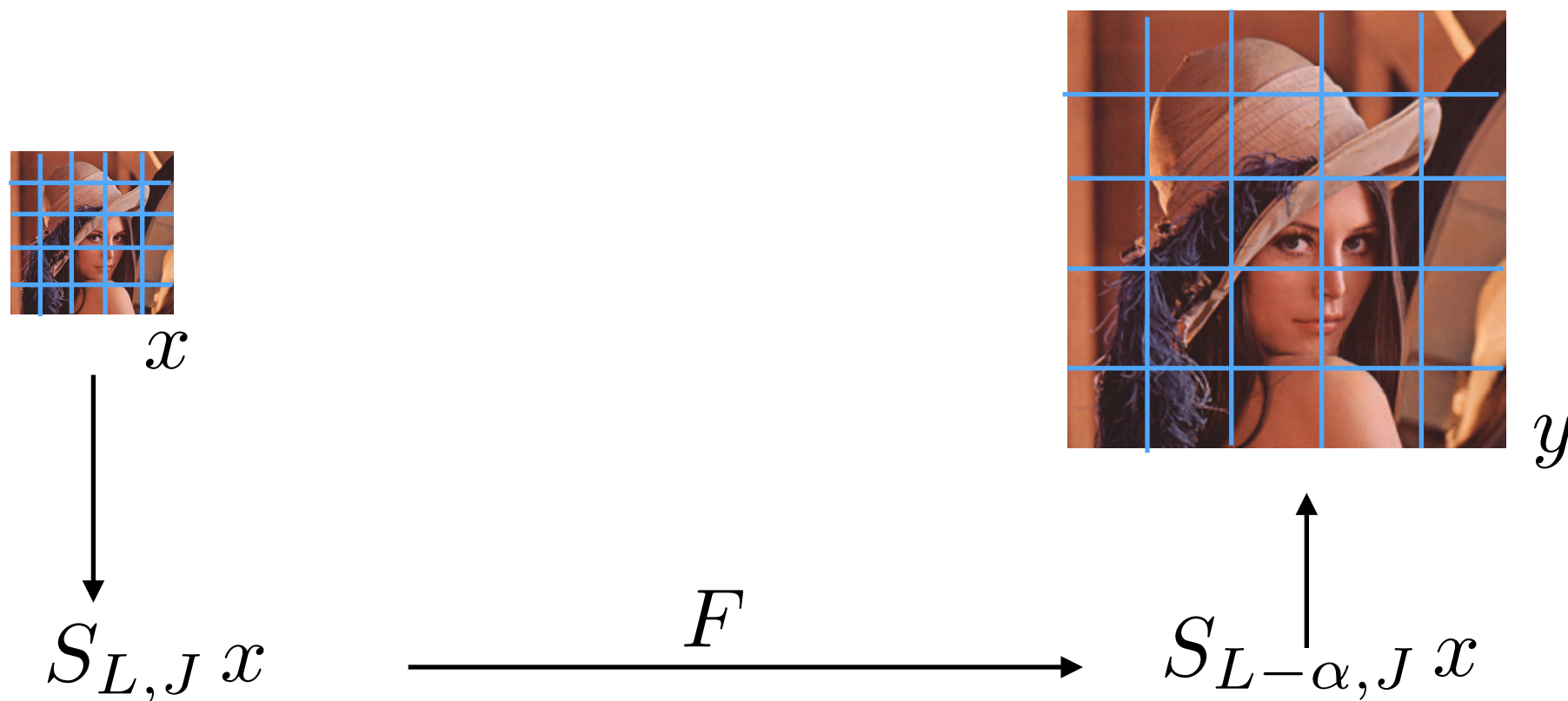
 y

- Best Linear Method: Least Squares estimate (linear interpolation):
- State-of-the-art Methods:
 - Dictionary-learning Super-Resolution
 - CNN-based: Just train a CNN to regress from low-res to high-res.
 - They optimize cleverly a fundamentally unstable metric criterion:

$$\hat{y} = (\hat{\Sigma}_x^\dagger \hat{\Sigma}_{xy})x$$

$$\Theta^* = \arg \min_{\Theta} \sum_i \|F(x_i, \Theta) - y_i\|^2 , \quad \hat{y} = F(x, \Theta^*)$$

Scattering Super-Resolution



$$S_{L,J}x = \begin{pmatrix} x \star \phi_{2^J}(u) \\ |x \star \psi_{j_1,k_1}| \star \phi_{2^J}(u) \\ ||x \star \psi_{j_1,k_1}| \star \psi_{j_2,k_2}| \star \phi_{2^J}(u) \end{pmatrix}_{L \leq j_1, j_2 \leq J}$$

- Linear estimation in the scattering domain
- No phase estimation: potentially worst PSNR
- Good image quality because of deformation stability

Super-Resolution Results

J. Bruna, P. Sprechmann



Original

Linear Estimate

state-of-the-art

Scattering

Super-Resolution Results

J. Bruna, P. Sprechmann



Original

Best
Linear Estimate

state-of-the-art

Scattering
Estimate

Super-Resolution Results

J. Bruna, P. Sprechmann



Original

Best
Linear Estimate

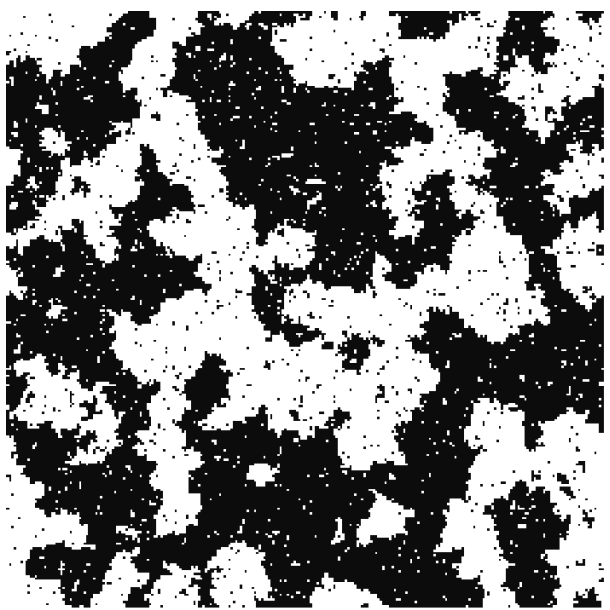
state-of-the-art

Scattering
Estimate

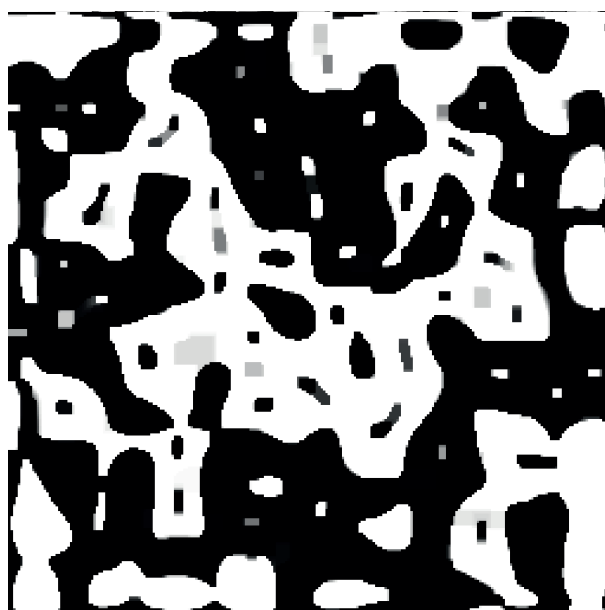
Super-Resolution Results

I. Dokmanic, J. Bruna, M. De Hoop

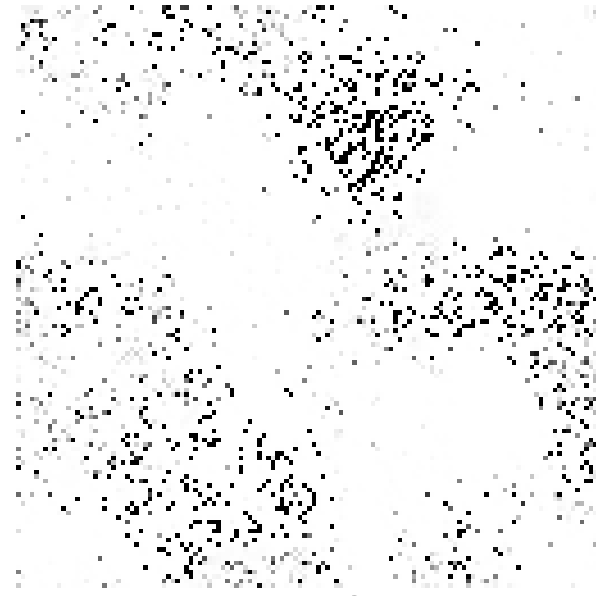
Original



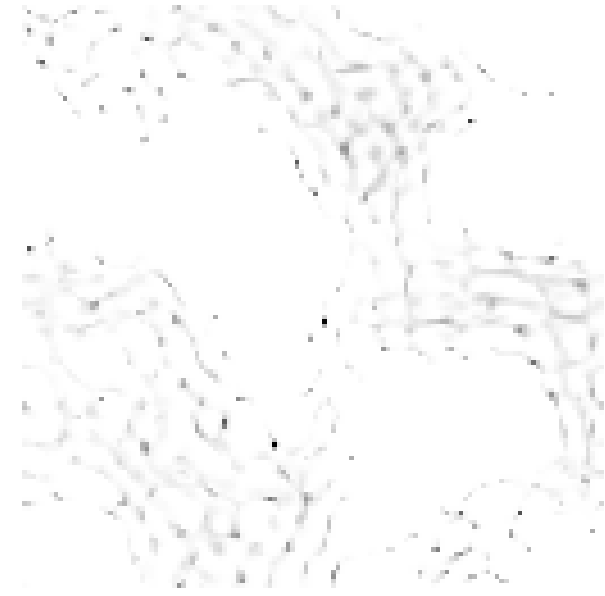
TV Regularization



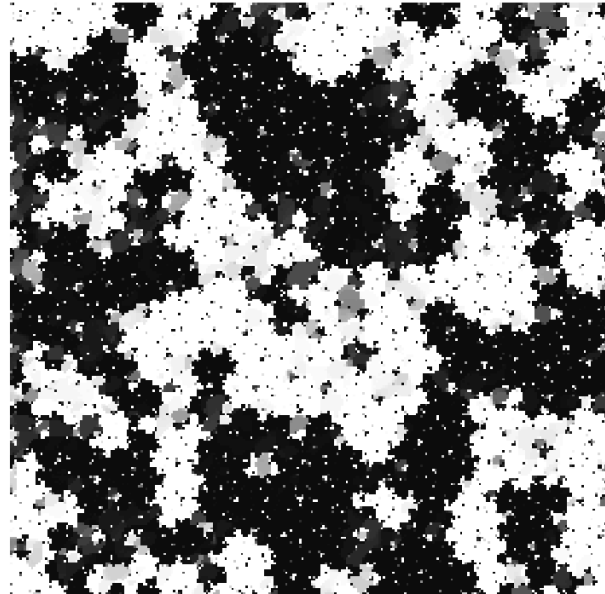
Original



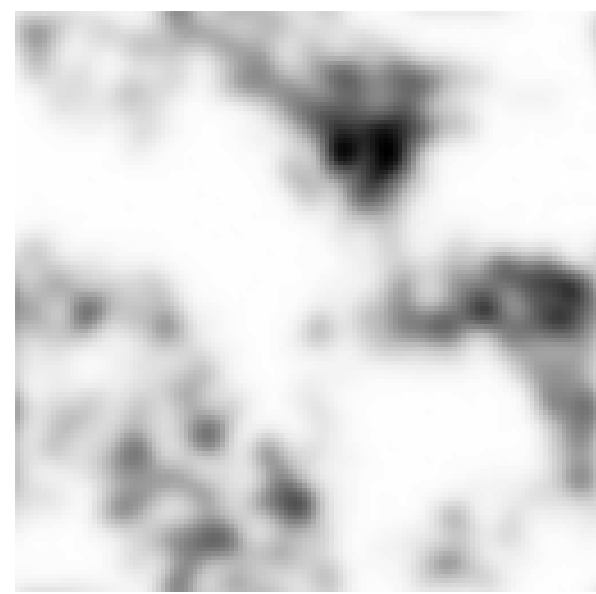
ℓ^1 Regularization



Low-Resolution



Scattering



Low-Resolution

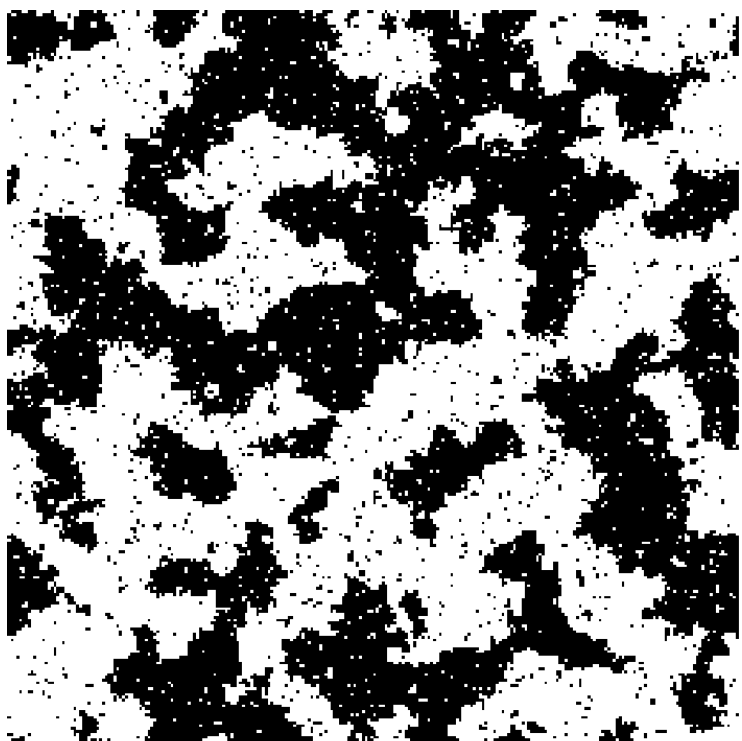


Scattering

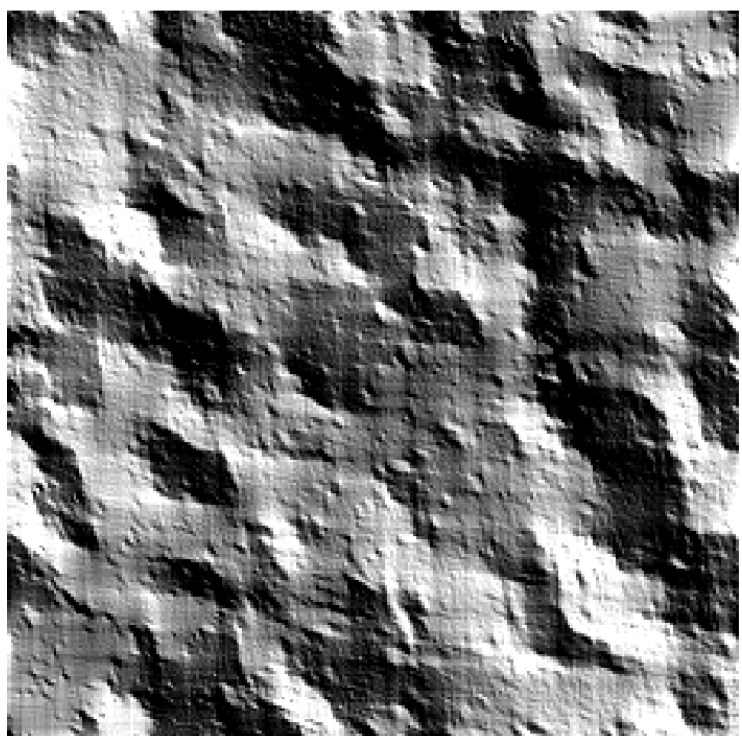
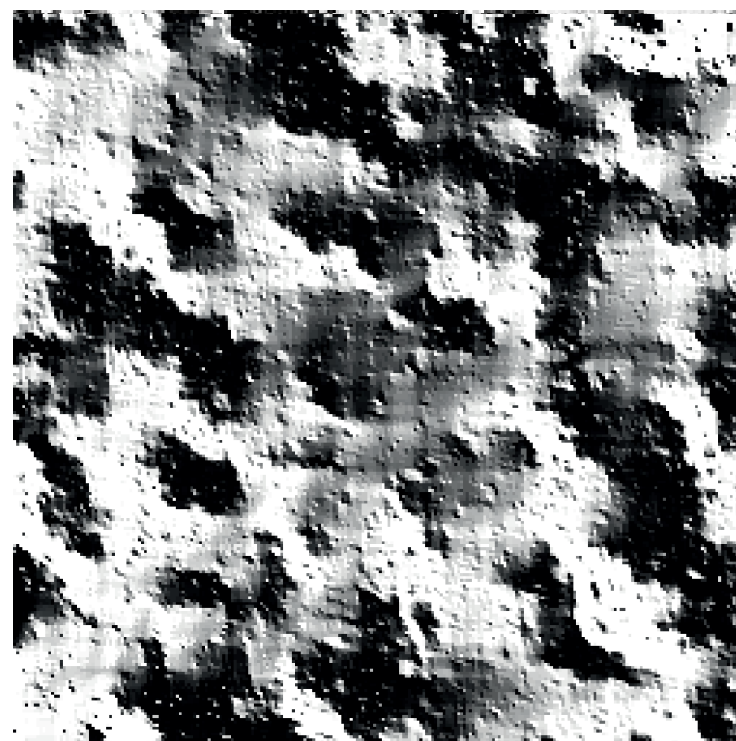
Tomography Results

I. Dokmanic, J. Bruna, M. De Hoop

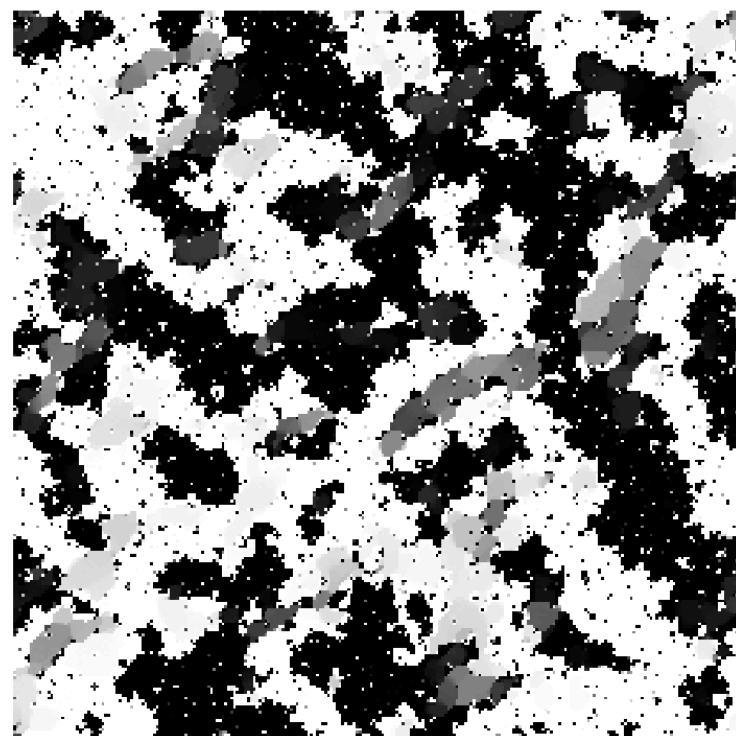
Original



TV Regularization



Low-Resolution



Scattering

Conclusions

- Deep convolutional networks have spectacular high-dimensional and generic approximation capabilities.
- New stochastic models of images for inverse problems.
- Outstanding mathematical problem to understand deep nets:
 - How to learn representations for inverse problems ?

(Not) Understanding Deep Convolutional Networks, arXiv 2016.